



## Antiphospholipid antibodies are enriched post-acute COVID-19 but do not modulate the thrombotic risk

Marc Emmenegger<sup>a,b,\*</sup>, Vishalini Emmenegger<sup>c</sup>, Srikanth Mairpady Shambat<sup>d</sup>, Thomas C. Scheier<sup>d</sup>, Alejandro Gomez-Mejia<sup>d</sup>, Chun-Chi Chang<sup>d</sup>, Pedro D. Wendel-Garcia<sup>e</sup>, Philipp K. Buehler<sup>e</sup>, Thomas Buettner<sup>f</sup>, Dirk Roggenbuck<sup>f,g,h,1</sup>, Silvio D. Brugger<sup>d,1</sup>, Katrin B.M. Frauenknecht<sup>i,j,1</sup>

<sup>a</sup> Institute of Neuropathology, University of Zurich, 8091 Zurich, Switzerland

<sup>b</sup> Division of Medical Immunology, Department of Laboratory Medicine, University Hospital Basel, 4031 Basel, Switzerland

<sup>c</sup> Department of Biosystems Science and Engineering, ETH Zürich, Basel, Switzerland

<sup>d</sup> Department of Infectious Diseases and Hospital Epidemiology, University Hospital Zurich, University of Zurich, Zurich, Switzerland

<sup>e</sup> Institute of Intensive Care Medicine, University and University Hospital Zurich, Zurich, Switzerland

<sup>f</sup> GA Generic Assays GmbH, Dahlewitz, Germany

<sup>g</sup> Institute of Biotechnology, Faculty Environment and Natural Sciences, Brandenburg University of Technology Cottbus-Senftenberg, Senftenberg, Germany

<sup>h</sup> Faculty of Health Sciences Brandenburg, University of Technology Cottbus-Senftenberg, Senftenberg, Germany

<sup>i</sup> Institute of Neuropathology, University Medical Center of the Johannes Gutenberg-University, 55131 Mainz, Germany

<sup>j</sup> National Center of Pathology (NCP), Laboratoire National de Santé (LNS), Luxembourg Center of Neuropathology (LCNP), 3555 Dudelange, Luxembourg

### ARTICLE INFO

#### Keywords:

Antiphospholipid antibodies  
Autoimmunity  
SARS-CoV-2  
Influenza  
Virology  
Cytokines  
Innate immunity  
Bayesian analysis  
Random forest regression  
Epidemiology

### ABSTRACT

**Background and objectives:** COVID-19-associated coagulopathy, shown to increase the risk for the occurrence of thromboses and microthromboses, displays phenotypic features of the antiphospholipid syndrome (APS), a prototype antibody-mediated autoimmune disease. Several groups have reported elevated levels of criteria and non-criteria antiphospholipid antibodies (aPL), assumed to cause APS, during acute or post-acute COVID-19. However, disease heterogeneity of COVID-19 is accompanied by heterogeneity in molecular signatures, including aberrant cytokine profiles and an increased occurrence of autoantibodies. Moreover, little is known about the association between autoantibodies and the clinical events. Here, we first aim to characterise the antiphospholipid antibody, anti-SARS-CoV-2 antibody, and the cytokine profiles in a diverse collective of COVID-19 patients (disease severity: asymptomatic to intensive care), using vaccinated individuals and influenza patients as comparisons. We then aim to assess whether the presence of aPL in COVID-19 is associated with an increased incidence of thrombotic events in COVID-19.

**Abbreviations:** AC, anticoagulation; AIC, Akaike information criterion; AnV, annexin V; aPL, antiphospholipid antibody; APS, antiphospholipid syndrome; AUC, area under the curve; ARDS, acute respiratory distress syndrome;  $\beta$ 2GPI,  $\beta$ 2-glycoprotein I; CI95%, 95% confidence interval; COVID-19, coronavirus disease 2019; CL, cardiolipin; CrI95%, 95% credible interval; CSS, cytokine storm syndrome; DPO, Day post onset of symptoms; ELISA, enzyme-linked immunosorbent assay; G-CSF, granulocyte colony-stimulating factor; GLM, general linearised model; GM-CSF, granulocyte-macrophage colony-stimulating factor; IgM, immunoglobulin M; IgG, immunoglobulin G; IgA, immunoglobulin A; IFN, interferon; IFN- $\alpha$ , interferon- $\alpha$ ; IFN- $\gamma$ , interferon- $\gamma$ ; IL, interleukin; IL-1 $\beta$ , interleukin-1 $\beta$ ; IL-4, interleukin-4; IL-6, interleukin-6; IL-8, interleukin-8; IL-10, interleukin-10; IL-17 A, interleukin-17 A; IP-10, IFN- $\gamma$ -induced protein 10; IQR, interquartile range; LASSO, least absolute shrinkage and selection operator; LIA, line immunoassay; MARS, multivariable adaptive regression spline; M $\phi$ , macrophage; MIP-1 $\alpha$ , macrophage inflammatory protein-1 $\alpha$ ; MIP-1 $\beta$ , macrophage inflammatory protein-1 $\beta$ ; NC SARS-CoV-2, nucleocapsid; OD, optical density;  $p(\text{EC}_{50})$ ,  $-\log_{10}(\text{EC}_{50})$ , the concentration at which half-maximum saturation is achieved; PA, phosphatidic acid; PC, phosphatidylcholine; PE, phosphatidylethanolamine; PG, phosphatidylglycerol; PI, phosphatidylinositol; PS, phosphatidylserine; PT, prothrombin; PAI, platelet aggregation inhibitor; PCA, principal component analysis; RBD SARS-CoV-2, receptor-binding domain; ROC curve, receiver operating characteristic curve; RT, room temperature; S100A8/A9, calprotectin; SARS-CoV-2, Severe acute respiratory syndrome coronavirus 2; SDF-1 $\alpha$ , stromal cell-derived factor-1 $\alpha$ ; Spike SARS-CoV-2, spike ectodomain; Th1, type 1 T helper cell; Th2, type 2 T helper cell; Th17, type 17 T helper cell; TMB, tetramethylbenzidine; TNF- $\alpha$ , tumour necrosis factor- $\alpha$ ; TRABI, tripartite automated blood immunoassay.

\* Corresponding author at: Division of Medical Immunology, Department of Laboratory Medicine, University Hospital Basel, 4031 Basel, Switzerland

E-mail address: [marc.emmenegger@usb.ch](mailto:marc.emmenegger@usb.ch) (M. Emmenegger).

<sup>1</sup> Shared senior authorship.

<https://doi.org/10.1016/j.clim.2023.109845>

Received 25 July 2023; Received in revised form 29 October 2023; Accepted 8 November 2023

Available online 22 November 2023

1521-6616/© 2023 The Authors. Published by Elsevier Inc. This is an open access article under the CC BY license (<http://creativecommons.org/licenses/by/4.0/>).

**Methods and results:** We conducted anti-SARS-CoV-2 IgG and IgA microELISA and IgG, IgA, and IgM antiphospholipid line immunoassay (LIA) against 10 criteria and non-criteria antigens in 155 plasma samples of 124 individuals, and we measured 16 cytokines and chemokines in 112 plasma samples. We additionally employed clinical and demographic parameters to conduct multivariable regression analyses within multiple paradigms. In line with recent results, we find that IgM autoantibodies against annexin V (AnV),  $\beta$ -2-glycoprotein I ( $\beta$ 2GPI), and prothrombin (PT) are enriched upon infection with SARS-CoV-2. There was no evidence for seroconversion from IgM to IgG or IgA. PT,  $\beta$ 2GPI, and AnV IgM as well as cardiolipin (CL) IgG antiphospholipid levels were significantly elevated in the COVID-19 but not in the influenza or control groups. They were associated predominantly with the strength of the anti-SARS-CoV-2 antibody titres and the major correlate for thromboses was SARS-CoV-2 disease severity.

**Conclusion:** While we have recapitulated previous findings, we conclude that the presence of the aPL, most notably PT,  $\beta$ 2GPI, AnV IgM, and CL IgG in COVID-19 are not associated with a higher incidence of thrombotic events.

## 1. Introduction

The prothrombotic phenotype observed predominantly in severe COVID-19, manifesting with venous thromboembolism, arterial occlusions, and diffuse coagulopathies, has been linked with APS, characterised by circulating aPL [1]. Over time, evidence that disturbances in the endothelial vasculature, a hyper-inflammatory immune response, and a state of hypercoagulability [2,3] are attributed to infection with SARS-CoV-2 has consolidated [4–8]. Some of the manifestations have been linked with the occurrence of symptoms post COVID-19 [9–12]. On the molecular level, a plethora of autoantibodies have been associated with acute or post-acute COVID-19 [1,13–17], of which few may be pathogenically relevant, including aPL [18–25]. While some have speculated whether the occurrence of aPL may be the link to hypercoagulability [26], some suggested that the thromboembolic features, including disseminated intravascular coagulation, triggered by infection with SARS-CoV-2 represented a secondary APS [27]. However, there has been little to no evidence that SARS-CoV-2 infection or its associated disease, COVID-19, can induce catastrophic APS [28] as the occurrence of aPL has not been sufficiently studied in the context of thrombotic events.

Here, in a heterogeneous cohort of 124 mixed-severity patients with multiple trajectories, we have generated a deep molecular profiling of factors associated with coagulation, including a panel of ten aPL assessed for three immunoglobulin isotypes, 16 inflammatory mediators (including cytokines and chemokines), and anti-SARS-CoV-2 antibodies. Importantly, we have included much needed control groups (which are often missing [29,30]), i.e., patients with acute infection with influenza and individuals after anti-SARS-CoV-2 mRNA vaccination, to contextualise and compare these results, as infections in general are known to trigger flares of autoimmune disease [31,32]. We found that IgM autoantibodies against AnV,  $\beta$ 2GPI, and PT are enriched upon infection with SARS-CoV-2. There was no strong supportive evidence for seroconversion from IgM to IgG or IgA. PT,  $\beta$ 2GPI, and AnV IgM as well as CL IgG antiphospholipid levels, significantly elevated in the COVID-19 but not in the influenza or control groups, were associated predominantly with the strength of the anti-SARS-CoV-2 antibody titres. Moreover, the major correlate for thromboses was SARS-CoV-2 disease severity. Overall, we conclude that while we observe a significant enrichment of aPL during acute and post-acute COVID-19, there is no evidence that COVID-19-associated aPL are responsible for the increased thrombotic

burden.

## 2. Material and methods

### 2.1. Study design and participants

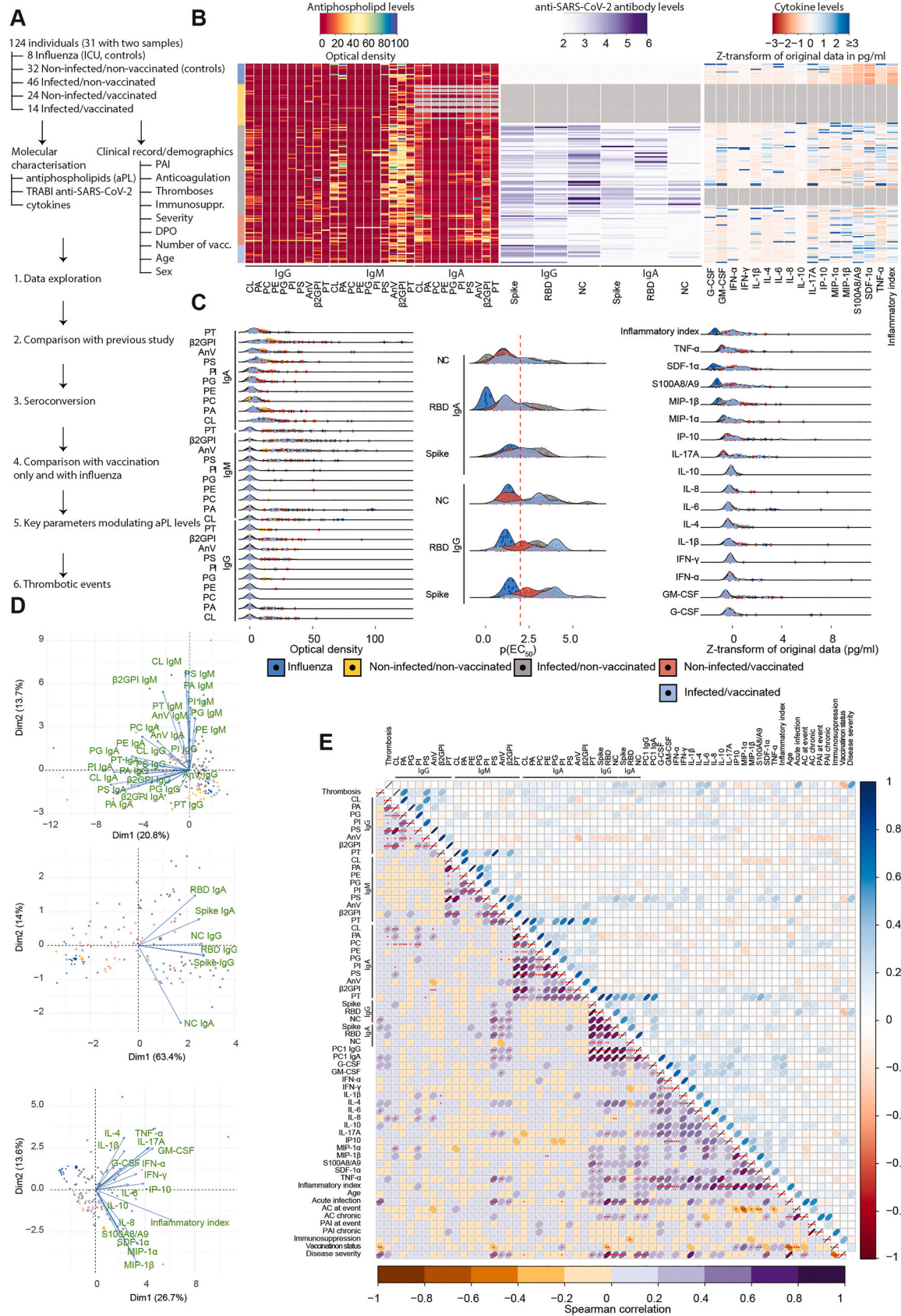
For this study, we included 124 patients (median age 58.0 (interquartile range (IQR): 39.0–69.0) years; distribution of female-male sex 0.444:0.556, see Table 1) admitted to the University Hospital Zurich, Zurich, Switzerland, from which we obtained 155 residual pre-omicron heparin plasma samples. Several patients ( $n = 49$ ) had previously been included in another study where antibody affinity against multiple SARS-CoV-2 RBD variants of concern (VOC) was investigated post infection or vaccination [33,34]. Other patients ( $n = 37$ , whereof 23 patients contributed two samples, i.e. total samples = 60) have been part of a study focused on superinfections in patients admitted to intensive care [35,36]; they are currently being investigated in the frame of a large multicentric collective to detail the anti-SARS-CoV-2 antibody kinetics in various biospecimens, alongside cytokines, upper and lower respiratory tract microbiota, and viral load. Furthermore,  $n = 8$  critically ill influenza patients (with two samples each) requiring intensive care have previously been part of a study investigating influenza [37] and their samples have been reused in the current framework to investigate aPL in two cohorts of acute-respiratory distress syndrome (ARDS) of different viral origins. For aPL-related analyses, to build a baseline, we have included 30 pre-pandemic individuals, complementing two other patients who have never contracted SARS-CoV-2 nor received a vaccination against SARS-CoV-2 at the time of sample donation (see Table 1). The samples of these patients, originally enrolled in multiple distinct studies, have therefore been ‘further used’ in the current study for the purpose of assessing the connection between the occurrence of aPL and the risk of experiencing thrombotic events. Moreover, for comparison, we have employed a dataset we had previously published [18]. The workflow of the study is depicted in Fig. 1A.

### 2.2. Ethics statement

All experiments and analyses involving samples from human donors were conducted with the approval of the ethics committee of the canton Zurich (KEK Zürich), Switzerland (KEK-ZH-Nr. 2015–0561, BASEC-Nr. 2018–01042, BASEC-Nr. 2020–01731, and BASEC-Nr. 2020-00646), in

**Table 1**  
Cohort characteristics.

	Influenza	Non-infected/non-vaccinated	Infected/non-vaccinated	Non-infected/vaccinated	Infected/vaccinated	Overall
Individuals, number	8	32	46	24	14	124
Samples, number	16	32	69	24	14	155
Median age (IQR)	54.5 (49.2 to 60.5)	28.5 (25.8 to 39.2)	62.5 (53.2 to 68.8)	67.0 (56.8 to 77.5)	73.5 (49.5 to 83.8)	58.0 (39.0 to 69.0)
Sex, female	4 (50.0%)	19 (59.4%)	16 (34.8%)	10 (41.7%)	6 (42.9%)	55 (44.4%)



(caption on next page)

**Fig. 1.** Study design, experimental approach, and data exploration. A. Study design and experimental approach. B-D. aPL, SARS-CoV-2 antibody, and cytokine heatmap (B), ridge plots to display the density distribution (C), and maximum variability projection in two dimensions using principal component analysis (D). Dark blue: influenza group. Yellow: non-infected/non-vaccinated. Grey: infected/non-vaccinated. Red: non-infected/vaccinated. Light blue: infected vaccinated. Within the heatmap, missing values (NA) are displayed in grey colour. E. Left triangle: Correlogram of all features. The Spearman regression coefficient is shown. Red asterisks indicate significance level; one asterisk indicates  $p$ -value  $< 0.01$ , and each additional one denotes a  $\log_{10}$  decrease. Right triangle: Choleski decomposition of square correlation matrix to assess collinearity of features within dataset. The diagonal indicates that almost all features contained in the dataset are non-collinear (while being correlated), except for AC, PAI, anti-SARS-CoV-2 antibodies, disease severity, PC1 IgG and PC1 IgA. PAI: platelet aggregation inhibitor. AC: anti-coagulation. TRABI: tripartite automated blood immunoassay. DPO: days post onset of symptoms. (For interpretation of the references to colour in this figure legend, the reader is referred to the web version of this article.)

accordance with the provisions of the Declaration of Helsinki and the Good Clinical Practice guidelines of the International Conference on Harmonisation. All subjects enrolled in the study signed the hospital-wide General Consent of the University Hospital Zurich, Switzerland and/or provided written Informed Consent [30].

### 2.3. High-throughput TRABI ELISA

Serological ELISAs were carried out using the tripartite automated blood immunoassay (TRABI) technology, as previously described [18,30,33] with minor adjustments. High-binding 1536-well plates (Perkin-Elmer; SpectraPlate 1536 HB) were coated with 3  $\mu$ l of 1  $\mu$ g/ml wildtype SARS-CoV-2 spike ectodomain (Spike), receptor-binding domain (RBD), or nucleocapsid (NC) protein in PBS using Fritz Gyger Certus Flex, incubated at 37°C for 1 h in a ThermoFisher rotating plate incubator, and washed three times with PBS 0.1% Tween-20 (PBS-T) using Biotek El406. Plates were blocked with 10  $\mu$ l of 5% milk in PBS-T for 1.5 h using Biotek Multiflo FX peristaltic dispensing technology. Samples inactivated with 1% Triton X-100 and 1% tributyl phosphate were diluted in sample buffer (1% milk in PBS-T), and a serial dilution (range: 0.02 to  $1.6 \times 10^{-4}$ ) was carried out (volume: 3  $\mu$ l per well) on an ECHO 555 acoustic dispenser (Labcyte) using contactless ultrasound nanodispensing. After the sample incubation for 2 h at RT, the wells were washed five times with wash buffer, and the presence of anti-SARS-CoV-2 antibodies was detected using horseradish peroxidase (HRP)-linked antibodies (1. anti-human IgG antibody: Peroxidase AffiniPure Goat Anti-Human IgG, Fc $\gamma$  Fragment Specific; Jackson; 109-035-098 at 1:4000 dilution. 2. anti-human IgA antibody: Goat Anti-Human IgA Heavy Chain Secondary Antibody, HRP; Thermo Fisher Scientific; 31417 at 1:750 dilution), all of them diluted in sample buffer at 3  $\mu$ l per well dispensed on Biotek Multiflo FX. The incubation of the secondary antibody for 1 h at RT was followed by three washes with PBS-T, the addition of 3  $\mu$ l per well of Tetramethylbenzidine (TMB) substrate solution with a Fritz Gyger Certus Flex dispenser, incubation of 3 min at RT, and the addition of 3  $\mu$ l per well 0.5 M H<sub>2</sub>SO<sub>4</sub> using Fritz Gyger Certus Flex. The plates were centrifuged in the Agilent automated microplate centrifuge after all dispensing steps, except for the addition of TMB. The absorbance at 450 nm was measured in a plate reader (Perkin-Elmer; EnVision), and the inflection points of the sigmoidal binding curves [i.e., the  $p(\text{EC}_{50})$  values of the respective sample dilution;  $p(\text{EC}_{50})$  is the negative logarithm of one-half the maximal concentration ( $\text{EC}_{50}$ )] were determined using a custom-designed fitting algorithm [30], with plateau and baseline inferred from the respective positive and negative controls in a plate-wise manner. Negative  $p(\text{EC}_{50})$  values, reflecting nonreactive samples, were rescaled as zero.

### 2.4. Measurement of autoantibodies against criteria and non-criteria phospholipid and phospholipid-related antigens

Line immunoassays (LIA; GA Generic Assays GmbH, Dahlewitz, Germany) for the detection of criteria and non-criteria aPL were used as previously described [18,38,39]. Briefly, plasma samples were analysed for IgG, IgA, and IgM against cardiolipin (CL), phosphatidic acid (PA), phosphatidylcholine (PC), phosphatidylethanolamine (PE), phosphatidylglycerol (PG), phosphatidylinositol (PI), phosphatidylserine (PS), annexin V (AnV),  $\beta$ 2-glycoprotein I ( $\beta$ 2GPI), and prothrombin (PT),

according to the manufacturer's recommendations. Diluted samples (1:33, in 10 mM TRIS with 0.1% Tween-20) were transferred onto LIA stripes, incubated for 30 min at room temperature (RT) while shaking. A 20 min wash step with 1 ml wash buffer (10 mM TRIS with 0.1% Tween-20) was used to remove unbound or loosely attached unspecific components from the LIA stripes. HRP-conjugated anti-human IgM, IgA, or IgG were incubated for 15 min at RT to bind to autoantibodies. After a subsequent wash step, 500  $\mu$ l of TMB were added to each LIA stripes as a substrate followed by drying the stripes for at least 30 min at RT. Optical density (OD) of processed strips were analysed densitometrically using a scanner and the corresponding evaluation software, Dr. Dot Line Analyzer (GA Generic Assays GmbH, Dahlewitz, Germany) with a grayscale calibration card for standardization provided with the kit. We have not used a binarization of the data into 'positive' or 'negative', according to a certain threshold, but looked at the distributions of ODs.

### 2.5. Cytokine measurements

Plasma cytokine levels were assessed using the Luminex MAGPIX instrument (ThermoFisher). Samples were thawed on ice and prepared according to the manufacturer's instructions using a custom-made 16-plex human cytokine panel (Procartaplex ThermoFisher), as shown [36]. In brief, Luminex magnetic beads were added to the 96-well plate placed on a magnetic holder and incubated for 2 min. The plate was washed twice with assay buffer for 30 s. In parallel, provided standards and plasma samples were diluted in assay buffer and added to the plate. The plate was incubated for 2 h at RT at 550 rpm in a plate orbital shaker. Next, the plate was washed twice with assay buffer and incubated for 30 min at 550 rpm with detection antibodies. After two washing steps, the plate was incubated with Streptavidin-PE solution for 30 min at 550 rpm. Finally, the plate was washed, reading buffer was added and incubated for 10 min at RT and 550 rpm before running the plate. Data acquisition and analysis were performed using the Xponent software (v. 4.3). Data were validated using the Procarta plex analyst software (ThermoFisher). The inflammatory index was calculated by (1) normalising the cytokine concentrations (z-score) and (2) by building the sum of the respective z-scores in a sample-wise fashion, thereby deriving a composite metric, as previously done [36]. Here, for the calculation of the inflammatory index, we used an independent dataset of 467 plasma samples of COVID-19 patients admitted to ICU, 50 plasma samples of patients with multiple trajectories (with or without history of infection with SARS-CoV-2, with or without SARS-CoV-2 mRNA vaccination, whose anti-SARS-CoV-2 immunoglobulin affinities have been characterised recently [33]), 16 samples of influenza patients with ARDS, and 24 plasma samples of patients admitted to ICU owing to severe burn injuries. Thus, the samples characterised in the frame of the current study represent a subset of the total on which the score was calculated. It is important to take note that for few (<5) patients with two timepoints but only one cytokine measurement, the cytokine measurement was reflected in both samples, i.e. duplicated. We aimed to avoid as many NA entries as possible as these interfere with subsequent analyses and models.

### 2.6. Collection of clinical parameters

Clinical parameters were collected using two in-hospital electronic

medical records databases, which included KISIM Version 5.0 (Cistec AG, Zurich, Switzerland) and Patient Data Management System (PDMS) MetaVision Version 6.1 (iMDsoft, Duesseldorf, Germany).

## 2.7. Quantification and statistical analysis

### 2.7.1. General statistical approaches

We display the actual  $p$ -values in the figures, regardless of whether the numbers are considered statistically significant or not (unless legibility in the figures is compromised) and indicate in the legend whether the values are corrected for multiple comparisons. Whenever indicated,  $p$ -values have been adjusted for multiple comparisons using Benjamini-Hochberg correction after conducting Wilcoxon rank sum tests on parametric as well as on non-parametric data. When reporting the median, we also document the interquartile ranges (IQR). Mean values are shown together with the standard deviation. For regression analyses, we document the 95% confidence interval (CI95%) for conventional frequentist-based regression and the 95% credible interval (CrI95%) for Bayesian regression. When conducting ordinary linear regression, the Spearman correlation coefficient  $R$  is shown. Throughout this study, the threshold value for significance,  $\alpha$ , is 0.01. However, the authors believe that hunting for significant  $p$ -values is counterproductive and partly responsible for the reproducibility crisis [40–43] and cannot compensate for assessing contextual and general biomedical relevance [40–46]. With this in mind, we have usually aimed to investigate the same problem from multiple viewpoints and have subsequently challenged our findings, to increase the stringency of our analyses. Additionally, in our analyses, although some variables may show a statistical effect, the threshold for them to be considered valid contributors to a phenotype is high as we require to observe strong evidence. In doing so, we avoid the overinterpretation of cohort-restricted small effects, since we look for relevant and generalisable effects. All analyses were conducted in R 4.2.2. Statistical testing was performed using the `ggpubr` package [44] and visualisations were performed almost exclusively with `ggplot2` [45]. Principal component analysis (PCA) and hierarchical clustering were conducted as shown [30,33]. When modelling data (shown below in Sections 2.7.2 and 2.7.3), we have refrained from employing a training and validation data set. Rather, we have trained the model on the entire data set to get the maximum precision from the given data – the parameters that went into the model had already been identified using multiple different approaches.

### 2.7.2. Feature selection of normally distributed outcome variables

Out of many molecular (e.g., IL-8), clinical (e.g., immunosuppression), and demographic (e.g., sex) parameters, we aim to identify those that correlate with our outcome variables. In one case, the outcome variable is an aPL value (e.g. PT IgM), which is based on a numeric scale from 0 to any natural number. The outcome variable here, therefore, is continuous and a conventional Gaussian general linearised model (GLM) can be employed to conduct multiple linear regression analysis. For feature selection, we have utilised random forest regression wrapped in Boruta [46] on Gaussian distributed data. We (1) run the Boruta algorithm for each outcome variable using all data and (2) used a dataset where we excluded aPL values  $\leq 1$ , to strengthen the identification of correlates of positivity. We then (3) compiled a list of all features considered important predictors according to Boruta, for each respective aPL, and (4) built a multivariable linear regression model in the form of

$$Y = \beta_0 + \beta_1 X_1 + \dots + \beta_n X_n + \varepsilon$$

where  $\beta_0$  is the Y intercept,  $\beta_i X_i$  the regression coefficient (i.e., slope) and the respective dependent variable, and  $\varepsilon$  the random error. (5) After this model was executed and the respective regression coefficients computed, we (6) additionally employed a step-AIC algorithm from the MASS library [47] to minimise the Akaike information criterion (AIC) by simplification of the model/selective removal of dependent variables,

$X_i$ . Next (7), we imported both modelling parameters based on the full model as well as the modelling parameters based on the AIC-improved model to predict the aPL level. We then (8) compared the observed/measured aPL value with the model-predicted aPL value and (9) used an ordinary linear regression to assess the quality of the prediction. Note that we selected features using random forest regression, harnessed the selected features in an ordinary Gaussian GLM, and then assessed the predictive power of the model, i.e. the selected parameters.

### 2.7.3. Feature selection of Bernoulli distributed outcome variables

We have been interested in assessing the possibility of the occurrence of correlates of thrombotic events. While in particular, we aimed to test the hypothesis that the occurrence of aPL is associated with the occurrence of thromboses (independent/outcome variable), we included a plethora of molecular, clinical, and demographic data other than aPL as predictor variables (dependent variables). The outcome, for each patient, was either 0 or 1, i.e., thrombosis = no or thrombosis = yes, and we have therefore employed models that work with Bernoulli distributions. Our strategy, overall, was to utilise several complementary approaches for feature selection, to then focus on those features having highest evidence of importance, to simplify and control the model in the best ways possible, and to use the model for prediction, whereby the goodness of the chosen parameters is evaluated. Along the procedure and by installing complementary approaches, we have been mindful about the issues of overfitting [48–51]. We started (1) with an ordinary Gaussian GLM, i.e., a multivariable linear regression, as for the binomial/Bernoulli GLM (multivariable logistic regression), the data did not converge. Linear and logistic regression are often interchangeable (for binary outcome variables) in terms of  $p$ -value outcome [52]. The first model, therefore, assumes the form shown in 2.7.2. The model was run on all data, on data where potentially collinear features have been removed, and on molecular data only (separately for aPL, SARS-CoV-2 antibodies, cytokines). Additionally, a step-AIC process was included, to further assess the data by aiming to focus on the ensemble of highest predictive character. Next (2), we aimed to stabilise the framework in which the regression is performed by employing Bayesian multivariable logistic regression with STAN [53], using the `rstanarm` [54] interface, as we have shown in other studies [30,55,56]. The utilisation of an unregularised prior (Normal(0, 10)), which led to a lot of noise in the estimates, was complemented by using a Bayesian LASSO and a regularised horseshoe [57] as shrinkage priors. We (3) performed a multivariate adaptive regression spline (MARS) analysis [58], using the earth package in R [59], tailored to binary outcome, as the modularity of the model might be suited to capture nonlinear relationships within the dependent variables. Ultimately, we (4) conducted a random forest regression with Boruta, as referred to before in Section 2.7.2. Then, we (5) selected the features for which the consensus to be of predictive importance was highest and (6) built several multivariable logistic regression models, in a bottom-up approach, starting with the most important parameter. In this bottom-up approach, we looked at the model parameters AIC and residual deviance, aiming to decrease both. Upon identifying the ‘best’ model according to AIC and residual deviance, we (7) generated multiple derivative models thereof, in addition to the ‘best model’: an AIC-improved model, a minimal model containing only the two most important features, an additional model containing those features that are not clearly related to those part of the minimal model, a cytokine model, and an aPL model. (8) All these models were then assessed in how well they predict the outcome, by comparing the predicted outcomes with the observed outcomes.

### 2.7.4. Code to all analyses and visualisations conducted in the frame of this study

The respective code describing the entire procedures, analyses, and visualisations is shown in the R script. Both the code as well as the visualisations, aiming to make scientific methods more Findable, Accessible, Interoperable and Reusable (FAIR) [60] as well as to bolster

**Table 2**  
Key resources used in this study.

Reagent or resource	Source	Identifier
<b>Antibodies</b>		
Goat anti-human IgG (1:4000 ELISA)	Jackson	109-035-098; RRID: <a href="https://doi.org/10.1016/j.isci.2023.105928">AB_2337586</a>
Goat anti-human IgA (1:750 ELISA)	Thermo Fisher Scientific	31417; RRID: <a href="https://doi.org/10.1016/j.isci.2023.105928">AB_228253</a>
Anti-human IgG (LIA)	GA Generic Assays GmbH	N/A
Anti-human IgM (LIA)	GA Generic Assays GmbH	N/A
Anti-human IgA (LIA)	GA Generic Assays GmbH	N/A
<b>Biological samples</b>		
Zurich COVID-19 ICU cohort		N/A
Zurich COVID-19 affinity cohort		N/A
Healthy blood donors		N/A
<b>Chemicals, Peptides, and Recombinant Proteins</b>		
WT SARS-CoV-2 Spike ECD	Introduced here [30]	<a href="https://doi.org/10.1016/j.isci.2023.105928">https://doi.org/10.1016/j.isci.2023.105928</a>
WT SARS-CoV-2 RBD	Introduced here [30]	<a href="https://doi.org/10.1016/j.isci.2023.105928">https://doi.org/10.1016/j.isci.2023.105928</a>
WT SARS-CoV-2 NC	AcroBiosystems	NUN-C5227
<b>Critical commercial assays</b>		
Procartaplex	ThermoFisher	N/A
aPL LIA	GA Generic Assays GmbH	N/A
<b>Software and algorithms</b>		
R 4.2.2 statistical software	R Core Team	N/A
R Studio 2022.07.1 Build 554	R Studio, PBC	N/A
Stan	Stan development team	N/A
Code deployed for this study	Zenodo repository [62]	Doi: <a href="https://zenodo.org/doi/10.5281/zenodo.10051978">https://zenodo.org/doi/10.5281/zenodo.10051978</a>

transparency to work against the plague of untrustworthiness quite prevalent in the medical field [61], are combined in an *R*markdown file, deposited on Zenodo [62].

## 2.8. Key resources used in the study

The most important resources used in the study are summarised in Table 2.

## 3. Results

### 3.1. Experimental approach, and data exploration

Thromboses are one of the globally leading causes of mortality [63] and COVID-19 has shown to predispose patients to thrombotic events [3]. Owing to manifest similarities of COVID-19-associated coagulopathy with the APS, aPL have been studied in some of the affected patients and, surprisingly, detected at higher frequency during acute or post-acute infection [20,21,24,64]. However, a causal connection between the occurrence of aPL and an increased thrombotic or thromboembolic burden has not been examined in depth. Here, we used a cohort of 124 individuals (31 with two samples, total number of samples = 155), with different exposures to SARS-CoV-2 and different disease severity, with or without vaccination (see Table 1 for population characteristics). For all of them, we have characterised their immunomolecular and clinical profiles to assess whether previous findings could be

**Table 3**  
Summary statistics aPL measurements.

	IgA	IgG	IgM	Overall
Measurements, number	1410	1550	1550	4510
Mean (STDEV)	8.1 (10.9)	2.4 (7.2)	9.4 (17.7)	6.6 (13.1)
Median (IQR)	5.0 (3.0 to 10.0)	0.0 (0.0 to 0.0)	0.0 (0.0 to 16.0)	0.0 (0.0 to 7.0)
Range	0 to 121	0 to 89	0 to 101	0 to 121

reproduced, to enhance the understanding on immunoglobulin seroconversion, and to investigate whether increased aPL levels might be a general feature post-viral infection or more specific to SARS-CoV-2. Moreover, we aimed to elucidate some of the molecular and clinical key parameters modulating aPL levels, and to identify potential correlates of thrombotic events (Fig. 1A). Details on thromboembolic complications are provided in Table S1 and include pulmonary embolism and stroke, e.g.

First, we aimed to look at the ensemble of molecular data with heatmaps (Fig. 1B) and distributional ridge plots (Fig. 1C). We sorted the individuals into five groups: (1) Influenza patients with critical illness sampled before the onset of the SARS-CoV-2 pandemic (dark blue), (2) non-infected/non-vaccinated patients (for SARS-CoV-2, yellow), (3) SARS-CoV-2 infected but non-vaccinated patients (grey), (4) patients who had never gotten infected with SARS-CoV-2 at the time of sampling but have received one or several vaccinations (red), and (5) patients following an infection with SARS-CoV-2 who had got vaccinated (light blue). aPL, measured using LIA for the detection of criteria and non-criteria aPL [18,38,39], displayed a high proportion of low ODs (see Table 3). In general, IgM aPL showed an inclination towards higher values in some patients or patient groups, notably CL, PA, AnV,  $\beta$ 2GPI, and PT (Fig. 1B and C). As supporting data in addition to aPL, we have characterised anti-SARS-CoV-2 Spike, RBD, and NC IgG and IgA in the cohort, using an approach introduced previously [30]. Patients with influenza or non-infected/non-vaccinated patients displayed  $p(\text{EC}_{50})$  values  $<2$ , i.e., titres reflecting an absence of reactivity, as expected (Fig. 1B and C, middle panel). Anti-SARS-CoV-2 NC reactivity was restricted to patients post infection and IgA appeared most pronounced in a subset of the infected/non-vaccinated group. To complement this molecular dataset, we assessed a panel of 16 important cytokines and chemokines, several of which have prothrombotic activity [65,66]. The z-transformed serum cytokine concentrations appeared quite heterogeneous, unlike the anti-SARS-CoV-2 IgG and IgA titres (Fig. 1B and C, right panel).

Principal component analyses mostly confirmed the impressions gained before (Fig. 1D). IgG and IgA aPL formed a big cluster, and another one was formed by IgM, while PT IgM and  $\beta$ 2GPI IgM clustered slightly apart (Fig. 1D, upper panel). Anti-RBD and anti-Spike IgG were almost identical and clustered together with anti-NC IgG, despite vaccination-only individuals having anti-Spike and anti-RBD titres without having anti-NC reactivity. Conversely, the anti-NC IgA profile contained a lot of information that was not covered with anti-RBD and anti-Spike IgA (Fig. 1D, middle panel). The cytokines largely clustered within two groups (Fig. 1D, lower panel). For aPL, anti-SARS-CoV-2 antibodies, and for cytokines, influenza patients as well as non-infected/non-vaccinated control patients typically clustered apart from the rest. Non-infected/vaccinated and infected/vaccinated usually fell in between, while infected/non-vaccinated individuals distributed non-focally, with opposite directionality.

As part of the first step in data exploration, we aimed to gain an understanding on the overall correlation contained within the parameters in our dataset, including the available clinical parameters for this study. We therefore plotted the Spearman correlation of all features (Fig. 1E, left triangle). Globally, we observed an extensive correlation within the same groups, e.g., IgG aPL correlated relatively well within



(caption on next page)

**Fig. 2.** Additional analyses performed on cytokines. A. Hierarchical clustering was performed on the cytokine data of patients with acute influenza or acute SARS-CoV-2 infection. Shown is the dendrogram for patients and the colour-coded groups. B. The same hierarchical clustering as in (A) was performed, with the dendrogram showing the cytokines, with colour-codes for three groups: Group 1: Chemokine, key pro-inflammatory, key anti-inflammatory, rest, compound (inflammatory index). Group 2: Th1, Th2, Th17, Th1/2, Th1/17, compound. Group 3: Pro-inflammatory, anti-inflammatory, anti- and pro-inflammatory, M $\phi$  and T cell recruitment, compound. C. Group-wise comparisons of cytokine plasma concentration. The individual measurements are indicated as dots, which are shown together with a conventional boxplot. Wilcoxon rank sum test with Benjamini-Hochberg correction for multiple comparisons was conducted and statistically significant changes are indicated in the figure. D. Same as in (C) but the cytokine plasma concentration is plotted against the time (day) at which the sample was collected post onset of symptoms (DPO). E. Using data from the current study as well as from an unpublished multicentric study on ICU COVID-19 patients and using data from literature [67–69], we compare cytokine levels in healthy controls, COVID-19 patients, influenza patients, vaccinated but non-infected controls, and in patients with primary CSS. A single dot reflects the mean concentration from a dataset (one study can contain multiple datasets for the same patient groups, see Table S2), which is displayed together with the standard deviation. If more than one mean value from one study is shown, a boxplot is displayed.

the group, while correlation outside the group was limited, and the same held true for almost all variables. We thus aimed to identify the exceptions: Thromboses correlated positively with anti-NC IgG and anti-Spike IgA, the linear combination of anti-SARS-CoV-2 IgG (termed PC1 IgG, see [18]), IL-6, acute infection, and mostly with disease severity; negative correlation with vaccination status manifested. Anti-SARS-CoV-2 antibodies, except anti-NC IgA, were positively correlated with IgM to AnV,  $\beta$ 2GPI, and PT. These three aPL were moreover positively correlated with IL-17 A, TNF- $\alpha$ , acute infection, and with disease severity. As we will subsequently use these parameters in multivariable regression models, we aimed to identify collinear features. We therefore conducted a Choleski decomposition on the correlation matrix using the Hermitian positive-definite matrix to identify features whose values approximate 0 (Fig. 1E, right triangle). We found that AC, PAI, anti-SARS-CoV-2 antibodies, and disease severity are partly collinear with other variables. PC1 IgG and PC1 IgA are markedly collinear, as expected. Collinearity can be a confounder in regression models and will be adequately addressed in subsequent chapters.

### 3.2. Investigation of cytokine profiles reveals differences between COVID-19 and influenza patients during acute infection

We have observed in Fig. 1C and D that the cytokine fingerprint in influenza patients appeared different from the rest, with low MIP-1 $\alpha$ , MIP-1 $\beta$ , S100A8/A9, SDF-1 $\alpha$ , TNF- $\alpha$  values, which was also reflected in a low inflammatory index, a compound metric recently introduced in the frame of COVID-19 [35,36]. Using all cytokine data available, we performed unsupervised hierarchical clustering on patients with an acute infection, i.e., with influenza or SARS-CoV-2, and colour-coded three groups: (1) Patients with influenza (dark blue), (2) infected but non-vaccinated patients (grey), (3) patients with infection and post vaccination (light blue). The result was in good agreement with the observation from the heatmap (Fig. 1B): while not being perfectly separated, the three groups formed distinct clusters (Fig. 2A). We then subjected the cytokines to hierarchical clustering, using three colour-coded readouts, differentiating (1, green-yellow colours) pro- and anti-inflammatory functionality, (2, purple colours) Th1, Th2, and Th17 groups, and (3, blue-orange colours) chemokines. Pro-inflammatory cytokines and chemokines like IL-6, GM-CSF, IL-17 A, TNF- $\alpha$ , IL-8, and SDF-1 $\alpha$  preferentially clustered together, while anti-inflammatory molecules like G-CSF, IL-10, or IL-4, and others with mixed effect (IFN- $\gamma$ ) did not form clear clusters (Fig. 2B). These analyses are suggestive that infection with influenza or SARS-CoV-2 lead to a differential cytokine release. Indeed, when statistically testing differences among the groups with patients suffering from an acute infection, for each of the cytokines as well as the inflammatory index, we identified significant differences only between non-vaccinated/vaccinated COVID-19 patients and influenza but not within COVID-19 patients (Fig. 2C), except for IL-4. S100A8/A9, SDF-1 $\alpha$ , MIP-1 $\beta$ , MIP-1 $\alpha$ , and the inflammatory index were significantly different from influenza, independent of the vaccination status (Wilcoxon rank sum test with Benjamini-Hochberg correction for multiple comparisons). Overall, we observed that the cytokine profiles remain relatively constant over time (Fig. 2D), indicating that the exact time of sample collection is likely not a principal

influence on the value measured. In a next step, we aimed to contextualise our results in comparison to previously published studies and datasets. We found four studies containing cytokine profiles of healthy individuals, COVID-19, influenza, and cytokine storm syndrome (CSS) patients. Three of them were used for subsequent comparison [67–69] and one was disregarded [70] as it only contained median and not mean concentration values. Additionally, we included our present dataset and data from an unpublished multicentre study conducted in ICU patients (see Table S2). Our main conclusions were that data from these mixed datasets were generally comparable, except for the cytokine profile of influenza patients which showed differences to ours in multiple instances (Fig. 2E).

### 3.3. Confirmation of key findings from previous study with new dataset

As we had conducted a multicentre study where we investigated the prevalence and association of aPL [18], we aimed to (1) challenge our previous results with the present cohort and (2) aimed to add to the previous study by detailing some aspects we had not been able to before. To enable a comparison, here, we restricted this first analysis to two patient groups: (1) non-infected/non-vaccinated ('no history of infection with SARS-CoV-2 or with vaccination against it until the time of sample donation'), and (2) infected/non-vaccinated, to exclude a potential bias induced by vaccination. As in the previous study, aPL IgA were not measured, we have not included information on IgA in this chapter.

Both female and male participants in the new and old cohorts showed a comparable age profile ( $p$ -values = 0.1 and 0.89, respectively, Wilcoxon rank sum test, Fig. 3A), and the female:male ratios were 0.449:0.551 in the new and 0.411:0.589 in the old cohorts (Table 4). The temporal variability in sampling was much more pronounced in this new cohort, with sampling being done at the day of onset of symptoms until >200 days post onset of symptoms (DPO), and significantly differed from the old cohort ( $p$ -value =  $1.8 \times 10^{-8}$ , Wilcoxon rank sum test, Fig. 3B). The composition of the cohort also differed regarding disease severity: while in the previous dataset, all severity categories (from 'no disease' to 'intensive care treatment') were covered to a similar extent, we observed a tendency towards no disease and most severe disease (Fig. 3C), with very few individuals who experienced mild-moderate COVID-19. When looking at the overall distributions of IgG and IgM aPL (Fig. 3D), we noticed that both in the new and old cohorts, the distributions of the non-infected/non-vaccinated and the infected/non-vaccinated differed significantly, except for IgM in the old cohort. We thus concluded that the current and previous cohorts differ in some important parameters.

We then aimed to investigate whether the key finding from the recent cohort, i.e., that PT in particular, but also  $\beta$ 2GPI and AnV IgM, but not IgG, were enriched in infected versus non-infected individuals [18], could be reproduced. While in the former study, we first conducted a Fisher's exact test (where all three antigens had higher IgM levels in the infected group) and then looked at the entire distribution (where only PT and  $\beta$ 2GPI but not AnV showed significant differences), we here directly compared the distributions using Wilcoxon rank sum test with Benjamini-Hochberg correction for multiple comparisons (Fig. 3E). As was the case in the previous dataset, PT and AnV IgG did not



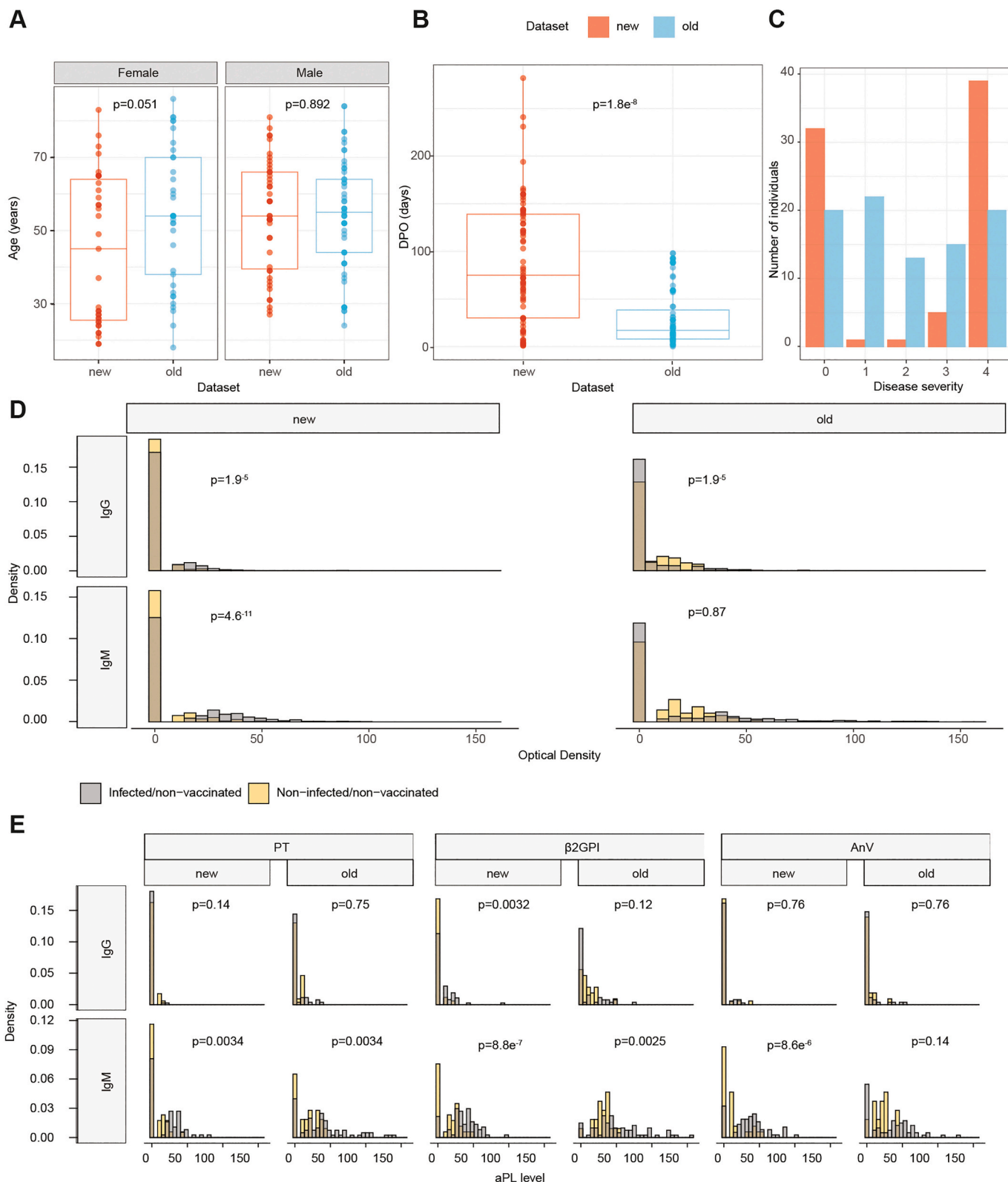


**Fig. 3.** Comparisons of findings between current and previous dataset. A. Comparison of age and sex between the previous study ('old') and current dataset ('new'). B. Comparison of day post onset of first SARS-CoV-2 symptoms (DPO) between previous study and current dataset. C. Comparison of COVID-19 disease severity between previous study and current dataset. D. Assessment of differences between SARS-CoV-2 infected and SARS-CoV-2 non-infected individuals regarding IgM and IgG aPL levels in previous study and current dataset. E. The same assessment as in (D), focusing on selected aPL that have shown distributional differences between infected and non-infected in the previous study. Wilcoxon rank sum test with Benjamini-Hochberg correction for multiple comparisons was conducted to test for distributional differences.

**Table 4**  
Comparison with previously published cohort.

	New cohort	Old cohort	Overall
Individuals, number	78	90	168
Samples, number	101	95	196
Median age (IQR)	53.5 (31.0 to 65.0)	54.0 (41.0 to 66.0)	54.0 (37.0 to 65.0)
Sex, female	35 (44.9%)	37 (41.1%)	72 (42.9%)
Non-infected/non-vaccinated	32 (41.0%)	20 (22.2%)	52 (31.0%)
Infected/non-vaccinated	46 (59.0%)	70 (77.8%)	116 (69.0%)

significantly differ between infected and non-infected groups. Yet,  $\beta$ 2GPI IgG was statistically different in the new dataset. We observed higher IgM levels for PT  $\beta$ 2GPI, and AnV in the new cohort ( $p$ -values between 0.0034 and  $8.8e^{-7}$ ). We therefore concluded that while the results were not fully congruent with the old dataset (as can be seen in Fig. 3E), the trend was reproduced. Even more importantly, PT IgM, which we focused on in the previous study, reproduced nicely, despite the differences in the cohorts used.

### 3.4. No evidence for seroconversion from IgM antibodies to IgA or IgG

One critique levied in the frame of our previous study [18] concerned the result that higher levels of IgM aPL, but not specifically of IgG aPL were identified. Covering a much wider range of DPOs (Fig. 3B) and additionally including IgA aPL, we aimed to reassess seroconversion and whether the occurrence of these IgM aPL antibodies are of transient nature. First, we were interested whether the overall IgA, IgG, or IgM aPL distributions differ among each other (Fig. 4A). Despite being largely overlapping, all the distributions differed significantly (all  $p$ -values  $< 0.0001$ ); the median IgA was 5.0 (mean: 8.1), IgG 0.0 (mean: 2.4), and IgM 0.0 (mean: 9.4), see Table 3. We then hypothesised that if there was seroconversion, we should observe a trend towards increased IgG and IgA with later DPO, and a potential decrease of IgM. We therefore conducted a linear regression on all data where DPO was available (i.e. non-infected/non-vaccinated and influenza patients were excluded). The Spearman correlation coefficient  $R$  was low for all Ig isotypes, close to 0, indicating constant titres over time (Fig. 4B). Conversely, this seemed to suggest the absence of seroconversion to IgA or IgG. As for some patients multiple time points were available, we decided to analyse them. A pairwise analysis indicated that mean IgA and IgM slightly increase at the second time point compared to the first one ( $p$ -values = 0.0078 and 0.00016, respectively, Wilcoxon rank sum test), while mean IgG slightly decreased ( $p$ -value = 0.89, see Fig. 4C), which did not solidify evidence for seroconversion. Lastly, we plotted the difference between the time points individually, for all samples, and modelled the behaviour using natural cubic spline functions [71,72], individually for all three isotypes (Fig. 4D). We used the range of the data as boundary knots and additionally used an internal knot at day 10, reflecting the 90th percentile in the data. While the spline for IgG reflected an approximated line, IgM and IgA displayed a slight increase with a peak somewhere between days 10-20, followed by a decline. Yet, the sum of evidence points against massive seroconversion from IgM to more long-lived IgG or IgA. On the other hand, IgM titres persisted over  $> 200$  days on the cohort level, which may hint that they are more than a transient phenomenon.

### 3.5. Infection with SARS-CoV-2, but not vaccination or infection with influenza, leads to increased IgM and IgG levels for select aPL

The post-acute-infection syndrome (PAIS), which might manifest as a heterogeneous group of symptoms, including fatigue, disturbed sleep, post-exertional malaise, and pain [11], is mechanistically understudied and occasionally confounded by the lack of an appropriate control group [29,30]. PAIS has been reported after infection with multiple viruses,

including cytomegalovirus [73], Epstein-Barr virus [73,74], influenza [75], and SARS-CoV-2 [33,76,77], and their pathogenesis may be owing to (1) persistent, yet undetected infection triggering a chronic immune response, (2) autoreactive disinhibited B or T cells within the frame of molecular mimicry, (3) or a dysregulation of the microbiome, virome, or mycobiome [11]. In particular, studies conducted in the last years suggested a surge in autoantibodies post COVID-19 [13–16], while other viral diseases have been less focused on. Here, we aimed to (1) characterise the aPL profiles in a heterogeneous cohort of patients with acute or post-acute COVID-19, (2) compare these profiles with influenza patients, (3) and further contrast these signatures with patients without a history of COVID-19 but who have received one or multiple mRNA vaccines against SARS-CoV-2. These analyses will help us understand whether aPL prevalence is increased specifically after an infection with SARS-CoV-2, or whether infection with another virus or a vaccine elicits a similar autoimmune phenotype. For this to be considered relevant, the distributions needed to (1) have a median change from baseline (the non-infected/non-vaccinated group)  $\geq 2$ , (2) have a median of  $\geq 10$ , and (3) a  $p$ -value  $\leq 0.01$ . The median change from baseline allows us to assess the effect of the change, rather than tiny distributional differences. The threshold of a median helps us to assess meaningful differences, rather than fluctuations close to ODs of questionable relevance. The  $p$ -value is derived from comparing the distributions with Wilcoxon rank sum test, hence, we only select differences that are statistically significant.

We first analysed the entire aPL distribution per isotype (and not individual aPL) and observed that none of the groups displayed relevant changes (Fig. 5A). However, when specifically evaluating individual aPL, we identified considerable changes of the infected/non-vaccinated group for PT IgM, AnV IgM,  $\beta$ 2GPI IgM, and CL IgG (Fig. 5B and Table 5). Such changes have not been evidenced for other aPL or for other patient groups, among them critically-ill patients suffering from influenza. This suggests that the signature observed here is a result of an infection with SARS-CoV-2. While mRNA vaccination combined with infection seem to diminish this signature, SARS-CoV-2 mRNA vaccination alone partially recapitulated the observations from the infection only group, for multiple aPL (Fig. 5B).

### 3.6. Identification of key parameters modulating aPL levels

Infection with SARS-CoV-2, and not with influenza, and to a lesser degree, vaccination with an mRNA vaccine, have shown to influence the occurrence of aPL autoantibodies in the former parts of this study. Here, we first plotted the respective ODs of all aPL against anti-SARS-CoV-2 IgG and IgA PC1, grouped into isotypes, and performed a linear regression (Fig. 6A), to see whether they are co-dependent. The Spearman correlation coefficient was  $< 0.14$  in all cases, which we interpreted as lack of evidence for a general driving of aPL titres by the strength of the anti-SARS-CoV-2 antibody response. However, PT IgM,  $\beta$ 2GPI IgM, AnV IgM and to a more limited extent CL IgG displayed some correlation with anti-SARS-CoV-2 PC1 IgG and IgA (Fig. 6B), even in the presence of a large number of OD = 0 values, forming a baseline. As in a recent study, we have revealed that IgM aPL against PT are associated with strength of the antibody response and are further modulated by COVID-19 disease severity, and sex [18,30,33], we here aimed to investigate potential modulators of PT, AnV,  $\beta$ 2GPI, and CL aPL. We therefore conducted random forest regression with Boruta, with PT IgM, AnV IgM,  $\beta$ 2GPI IgM, and CL IgG as the respective dependent variables and a plethora of clinical, demographic, and molecular parameters (see *Rmarkdown* file on Zenodo [62]) as independent variables. The analyses were performed twice, on all data points and after selecting individuals with OD  $> 1$ , thereby excluding OD  $\leq 1$ . We obtained lists of the features considered important according to random forest regression (Table 6) and employed all of them in a conventional general linearized model. Additionally, we conducted an automated Akaike information criterion (AIC) improvement to simplify the model as much as possible, aiming to

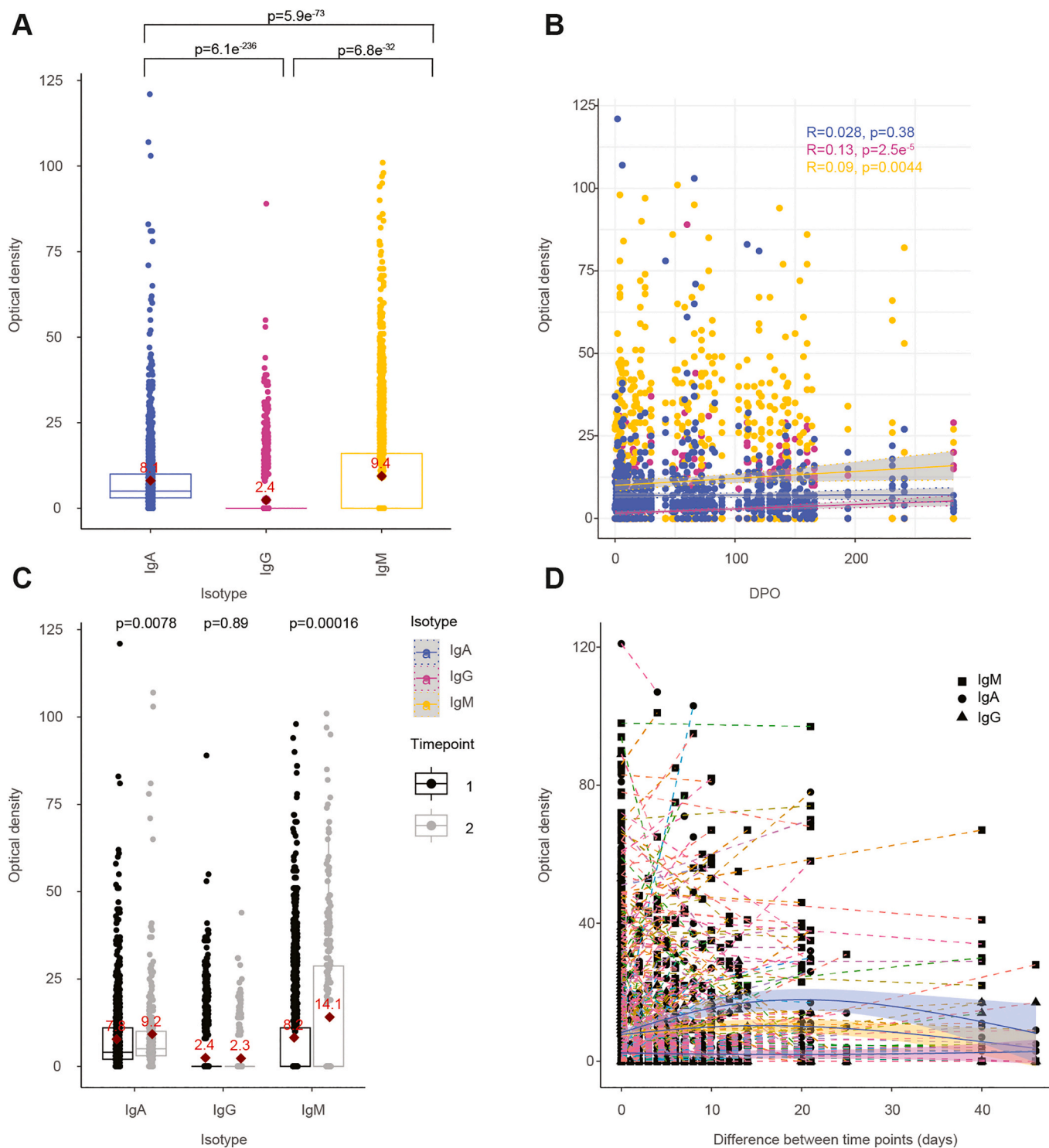


**Fig. 4.** No evidence for seroconversion from IgM antibodies to IgA or IgG. **A.** Boxplot with individual dots representing aPL measurements performed on all aPLs, shown for distinct isotypes. In addition to the boxplot, the mean value of each isotype is shown in red. *P*-values were calculated with Wilcoxon rank sum test and Benjamini-Hochberg corrected for multiple comparisons. **B.** Same values as in (A) for which DPO is available. Spearman correlation coefficients calculated for each isotype indicate no linear trend between aPL ODs and DPO. **C.** For patients for which two timepoints were available, we compared the first and the second timepoint, for each isotype, without splitting into individual aPL. Both IgA and IgM, but not IgG, displayed a tendency for increased values at the second time point. Wilcoxon rank sum test was conducted to test for distributional differences. **D.** For patients used in (C), the difference between the time points were plotted. The trends between the measurements from the same patient, split into individual aPL and antibody isotype. The trends are displayed by using a natural cubic spline function, following the same colour-code as above. (For interpretation of the references to colour in this figure legend, the reader is referred to the web version of this article.)

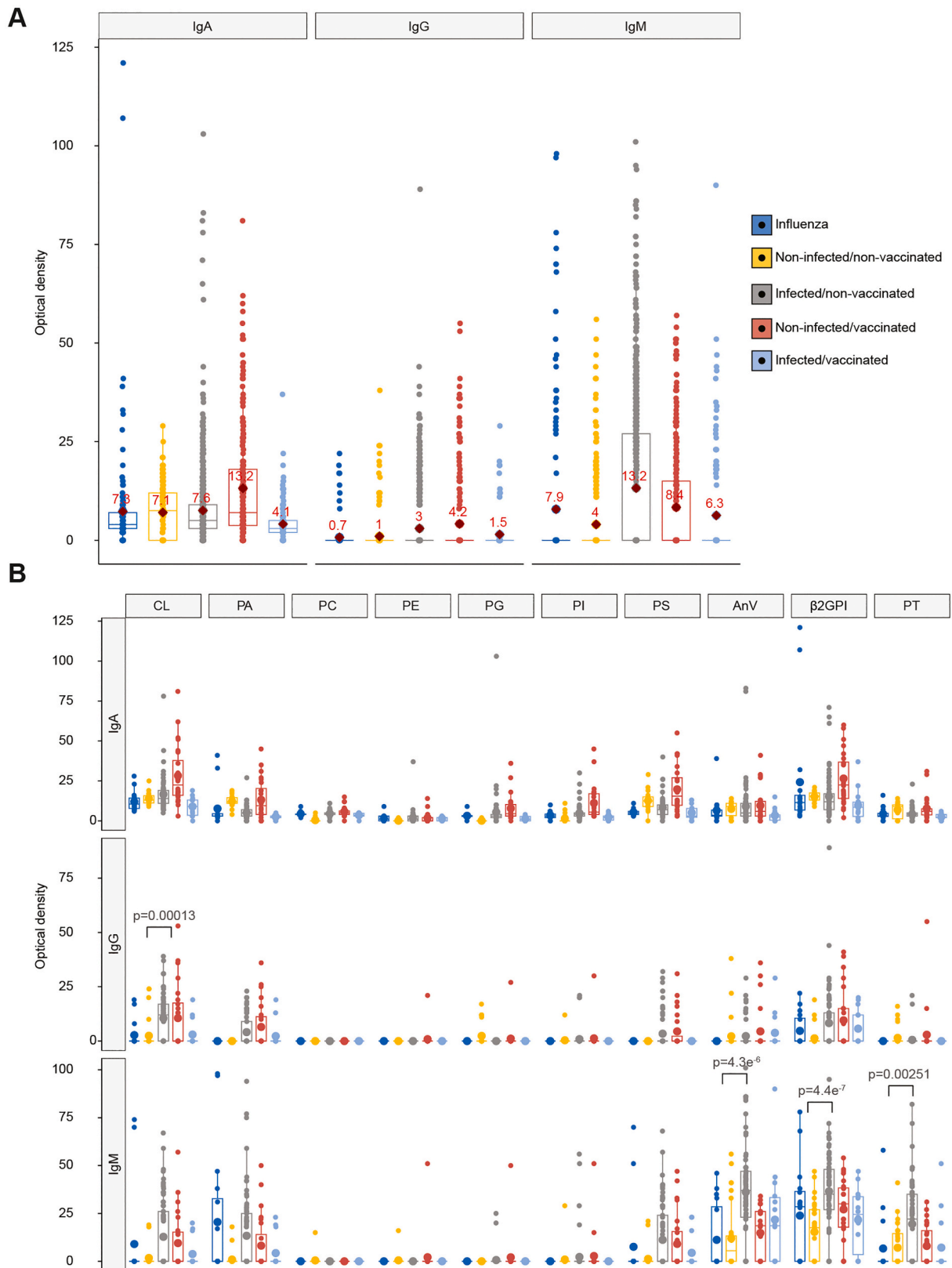


**Fig. 5.** Infection with SARS-CoV-2, but not vaccination or infection with influenza, leads to increased PT,  $\beta$ 2GPI, and AnV IgM, and CL IgG levels in the infected-only group. A. Comparison of all aPL isotypes, by groups. We applied the following criteria for identification of differences: (1) We only consider groups with median change from baseline  $\geq 2$ , (2) with a median of  $\geq 10$ , and (3) with p-value  $\leq 0.01$ . The median change from baseline allows us to assess the effect of the change, rather than tiny distributional differences. When looking at all aPL together, none of the groups displayed a change according to above definition. B. Same as in (A), but the analysis is separated for individual aPL levels. The infected-only group showed relevant changes for PT,  $\beta$ 2GPI, and AnV IgM, and CL IgG.

**Table 5**

aPL levels compared to baseline. We conducted comparisons to assess whether the distributions and the effects differ among the groups. We compared the distributions of all groups against baseline, i.e. non-infected/non-vaccinated. We applied the following criteria for identification of differences: (1) We only consider groups with median change from baseline  $\geq 2$ , (2) with a median of  $\geq 10$ , and (3) with  $p$ -value  $\leq 0.01$ . The median change from baseline allows us to assess the effect of the change, rather than tiny distributional differences. The threshold of a median helps us to assess meaningful differences, rather than fluctuations close to ODs of questionable relevance. The  $p$ -value is derived from comparing the distributions with Wilcoxon rank sum test, hence, we only select differences that reach statistical significance.

Patient group	aPL	Median (IQR)	Median change from baseline	p-value
Infected/non-vaccinated	PT IgM	22.0 (0.0-35.0)	Infinite	0.00251
Infected/non-vaccinated	AnV IgM	37.0 (23.0-47.0)	6.73	4.3e <sup>-06</sup>
Infected/non-vaccinated	$\beta$ 2GPI IgM	35.0 (27.0-48.0)	2.00	4.4e <sup>-07</sup>
Infected/non-vaccinated	CL IgG	12.0 (0.0-17.0)	Infinite	0.00013

obtain the most relevant parameters. Using the full (Fig. 6C) or the AIC improvement model (Fig. 6D), we then predicted the respective aPL values, to assess the predictive quality of our model. While the utilisation of the full model generally led to the best Pearson correlation coefficient, we observed that the AIC simplified models predicted the aPL ODs quite nicely, with  $R \geq 0.52$  in all cases. This suggested that NC IgG, together with MIP-1 $\alpha$ , IL-8, and age are associated with PT IgM titres (Table 6). AnV IgM is associated with NC IgG, disease severity, IL-17 A, and age and  $\beta$ 2GPI IgM is associated with NC IgG and IgA, SDF-1 $\alpha$ , and IL-4. CL IgG is associated with PC1 IgG, Spike IgA and IgG, NC IgG, IL-8, SDF-1 $\alpha$ , and age. When building a model for PT IgM with ‘immunosuppression’ alone, with age only, or with sex only (Fig. 6E), any predictive value vanished. The predicted values for PT IgM based on the age model was additionally plotted against the observed values of PT IgA (see Fig. 6E, third panel) and unlike in all other models, the y-intercept  $\beta_0 \neq 0$  and the slope  $\beta_1 \neq 1$ , as the modelled values (for IgM) are based on observations different from the ones shown here (IgA). These controls display that valid predictions do not accrue from non-informative parameters. Conversely, they validate that the selected candidates are associates of aPL reactivity. Thus, the strength of the antibody response against SARS-CoV-2 and particularly the IgG response against NC, which displays an excellent correlation with disease severity (see Fig. 1E), is a key modulator of the respective aPL. Additionally, chemokines and cytokines, notably MIP-1 $\alpha$ , SDF-1 $\alpha$ , IL-4 and IL-8, and age contribute to the effect. This result, obtained within an entirely new cohort, validates, and extends our previous observation [18].

### 3.7. Thrombotic events are associated with SARS-CoV-2 disease severity, while evidence for association with any aPL is limited

COVID-19-associated coagulopathy entails an increased risk of developing thromboses and is reminiscent of the antiphospholipid syndrome [20,26,78,79]. As many groups have reported higher aPL levels in COVID-19 [21,24,25,64,80], including in this study where we have additionally compared COVID-19 with influenza, a ‘never infected’ group and individuals after receiving vaccinations, it could be hypothesised that thrombotic events following COVID-19 are triggered by aPL. As the information whether patients included in our study have developed thromboses was available, we were able to experimentally evaluate whether increased aPL levels, or other variables included in our dataset, have a higher propensity to elicit thrombotic events. However, the large numbers of covariates required a careful assessment. We have therefore used multiple modalities for the initial process of identifying

potentially important parameters. We first employed ordinary multi-variable linear regression on all data, on data after removing collinear features (see Fig. 1E, Choleski decomposition), and on aPL, SARS-CoV-2 antibodies, and cytokines only (adjusted for age and sex) and plotted the exponentiated regression coefficients with 95% confidence intervals (CI95%), displayed in Fig. 7A. After accounting for collinearity, we found disease severity, anti-NC IgG anti-NC IgA as well as anti-Spike IgG and IgA to be fairly higher (see Table 7), also when running an AIC improvement (colour-coded in the plot, as detailed in the figure legend). While running a linear regression instead of logistic regression on data with binary outcome can sometimes be legitimated [52], our reason for doing so was the non-convergence of the fits, which resulted in a large uncertainty so that no reliable estimate of the regression coefficients could be obtained. To make regression more stable, we have employed multivariable logistic regression in a Bayesian framework [30,54–56]. Using an unregularised as well as a LASSO and a regularised horseshoe approach, we identified disease severity as the most important correlate of thrombosis (OR:2.98, CrI95%: 1.80-5.81), and additionally perhaps IL-6, and SDF-1 $\alpha$ , the latter being negatively correlated (Fig. 7B and Table 7). The predictions of the MARS model were in good agreement as disease severity was ranked as the most important feature, followed by anti-SARS-CoV-2 antibodies and some cytokines (Fig. 7C and Table 7). Random forest regression with Boruta, which assesses the importance of each predictor variable independently rather than conducting multivariate regression, identified disease severity as the most associated parameter (Fig. 7D and Table 7) with thrombosis and additionally anti-SARS-CoV-2 antibodies, some cytokines (G-CSF, IL-6, IP-10, IL-4, SDF-1 $\alpha$ , IL-10), and  $\beta$ 2GPI IgM, the only aPL to appear in all these analyses. Based on findings of these analyses, we have then aimed to select the best combination of these parameters, to predict the outcome most accurately. Starting with those features where highest consensus was reached (i.e. disease severity), we added more features, one after the other, and assessed modelling parameters (AIC and residual deviance), aiming to minimise the two. This resulted in a logistic regression model consisting of multiple parameters (Fig. 7E), which we refined using an AIC improvement algorithm. Moreover, we also generated a minimal model where only two parameters, disease severity (largely correlated with anti-SARS-CoV-2 antibodies, see Fig. 7E) and NC IgA (least correlated with disease severity, or with other anti-SARS-CoV-2 antibodies), were considered. An additional model was built accounting for parameters included in the best model but not included in the minimal model, i.e. cytokines and  $\beta$ 2GPI IgM. In the cytokine model, we additionally removed  $\beta$ 2GPI IgM and in the aPL model, we only included  $\beta$ 2GPI IgM. For all models, we then compared the observations (absence or presence of thrombosis) with the calculated probability, i.e. the predicted values (Fig. 7F). The best and the AIC improved models predicted the outcome quite well, at 92.0 and 91.1%, respectively. When only using disease severity and NC IgA titres (minimal model) as parameters, we still predicted 83.0% of outcomes correctly. The additional model, the cytokine model, and the aPL model all lost predictive power, as can be seen when looking at the ROC curves (Fig. 7G). The aPL model is random (AUC: 0.522), and the additional and the cytokine models are close to being unusable (AUC: 0.728 and 0.729, respectively). Disease severity and NC IgA alone (AUC: 0.830) already have a marked predictive capacity, while the more complex models add further strength (AUC  $\geq 0.929$ ). First and importantly, these results do not support that the occurrence of aPL are correlated with, and potentially cause, thromboses. However, the data is suggestive that disease severity and a proxy of it, the strength of the anti-SARS-CoV-2 antibody response, are associated with thromboses. Additionally, G-CSF, which is known to induce thrombocytopenia and IL-6, a documented risk factor for coagulopathies [3], display an association although by themselves, their associations are weak.

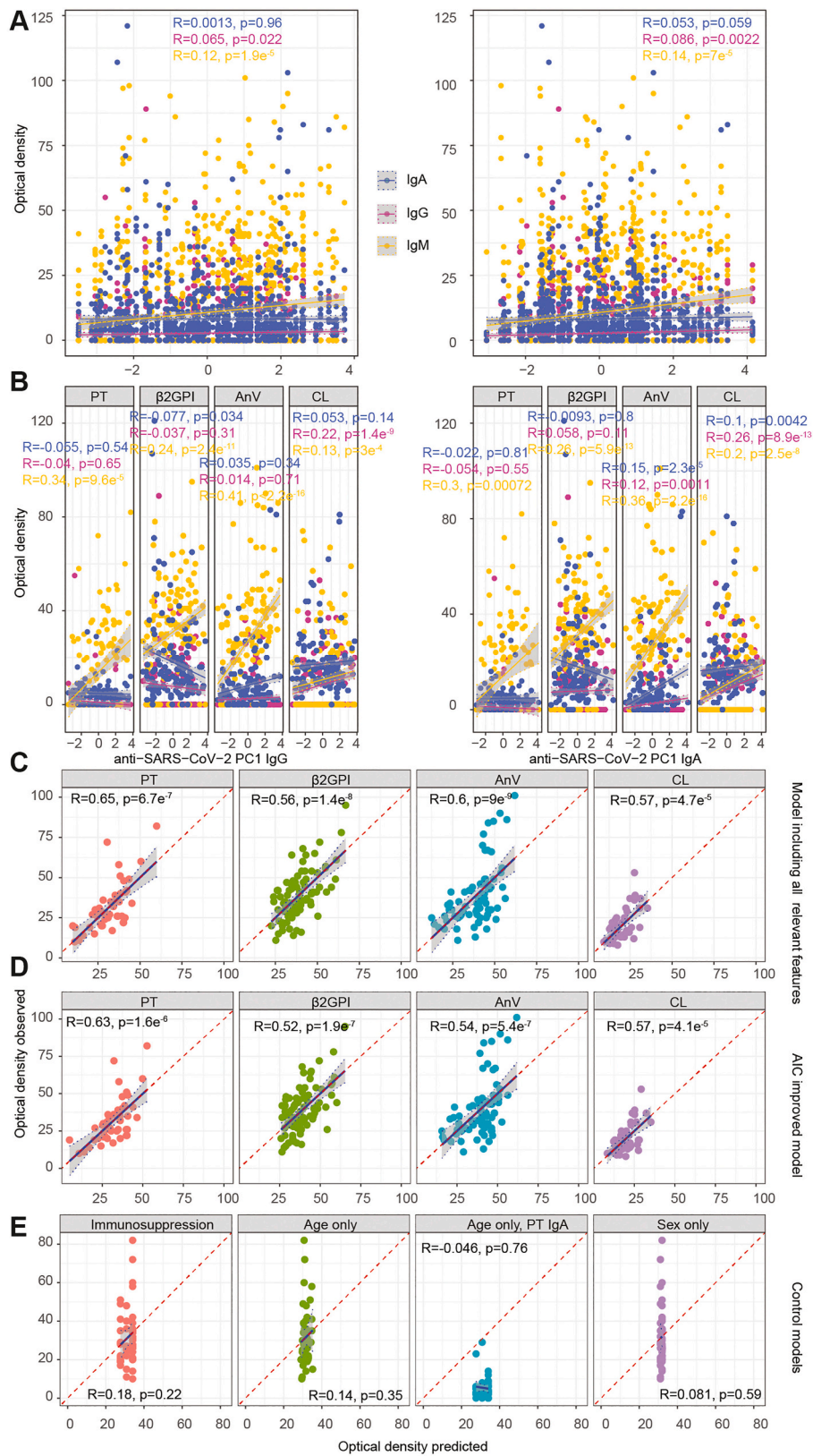


**Fig. 6.** Identification of key parameters modulating aPL levels. A. aPL levels are not generally modulated by the strength of the antibody response against SARS-CoV-2 proteins, neither IgG (left) nor IgA (right). The first PC of the SARS-CoV-2 TRABI measurements are displayed. B. PT, beta2GPI, and AnV IgM, but not IgG or IgA, are modulated by the strength of the antibody response against SARS-CoV-2 proteins, as shown previously. Additionally, CL IgG appears slightly correlated with the strength of the antibody response. C-E. Regression model to infer predictors of aPL levels. Features were identified using random forest regression and then used to model the respective aPL response. The full model behaviour (prediction versus actual observation) is shown (C), the AIC-improved model in (D), and control models in (E). While all models in (C) and (D) contain valuable information, the models shown in (E) display that the utilisation of non-informative parameters leads to a lack in predictive capacity.

**Table 6**  
List of features predicting select aPL levels.

aPL	Identified with Boruta and used in GLM	After AIC improvement
PT IgM ~	NC IgG, PC1 IgG, disease severity, vaccination status, acute SARS-CoV-2 infection, TNF- $\alpha$ , S100A8/A9, IP-10, IL-8, age, MIP-1 $\alpha$ , Spike IgA, RBD IgG	NC IgG, MIP-1 $\alpha$ , IL-8, age
AnV IgM ~	NC IgG, PC1 IgG, RBD IgA, PC1 IgA, disease severity, acute SARS-CoV-2 infection, age, TNF- $\alpha$ , IL-17 A, vaccination status, IL-4	NC IgG, IL-17 A, disease severity, age
$\beta$ 2GPI IgM ~	NC IgG, NC IgA, RBD IgA, disease severity, vaccination status, age, IL-4, TNF- $\alpha$ , SDF-1 $\alpha$ , IL-17 A, age, MIP-1 $\alpha$ , PC1 IgG	NC IgG, NC IgA, SDF-1 $\alpha$ , IL-4
CL IgG ~	NC IgG, Spike IgG, PC1 IgG, RBD IgA, Spike IgA, PC1 IgA, IL-8, IL-4, MIP-1 $\alpha$ , SDF-1 $\alpha$ , age	PC1 IgG, Spike IgA, Spike IgG, IL-8, NC IgG, SDF-1 $\alpha$ , age

#### 4. Discussion

Many of the coagulation-associated features of COVID-19 pathology, particularly the formation of micro- and macrothrombi, are reminiscent of the catastrophic APS [2,22,28]. In parallel, a large body of evidence supports an enrichment of aPL during acute or post-acute COVID-19 [19–21,24–26,28,64], and total IgA and aPL-specific IgA were associated with severe illness [81]. Thus, one may speculate that the occurrence of aPL after infection with SARS-CoV-2 is causatively connected with APS-like COVID-19-associated coagulopathy.

First, our results confirmed previous observations, including our own [18], as we reported a significant enrichment of both IgG and IgM aPL in infected (non-vaccinated) versus non-infected (non-vaccinated) individuals. When looking into the granularity of the data, we had not been interested in observing merely statistical fluctuations but aimed to identify biologically relevant effects. To this end, we have set stringent criteria when comparing individual aPL levels between groups. While observing a trend for increased aPL levels in individuals after vaccination only (in the absence of a history of infection with SARS-CoV-2), we identified the most notable enrichments in patients with acute or post-acute SARS-CoV-2 (without a history of vaccination) but not with acute influenza, for PT IgM, AnV IgM,  $\beta$ 2GPI IgM, and CL IgG. While no other significant effect was found, PA (IgG and IgM), CL (IgM and potentially IgA), and PS (IgG and IgM) displayed a similar trend – for infected only and for vaccination only groups – and might be considered relevant if the cohort size was further enlarged. We interpreted this result as a suggestion that aPL levels are not generally elevated upon any viral infection but that there is some level of specificity, and that some but not other aPL are increased. Interestingly, this difference between infection with SARS-CoV-2 and with influenza was complemented by a distinct cytokine profile, which we have further visualised using PCA and hierarchical clustering. S100A8/A9, SDF-1 $\alpha$ , MIP-1 $\beta$ , MIP-1 $\alpha$ , TNF- $\alpha$ , and likely also GM-CSF displayed markedly distinct distributional patterns in acutely infected influenza and COVID-19 patients. They are all mainly produced by Th1 or Th17 T helper cells as well as by macrophages and promote an inflammatory environment [82] that may result in an acute respiratory distress syndrome (ARDS), a core feature of severe COVID-19. While the classical signatures of the cytokine storm syndrome were largely absent in COVID-19 patients, an observation shared with others [68], our data is suggestive of significantly altered cytokine signalling in acute COVID-19 compared with acute influenza. However, a limitation of these comparisons among cohorts contained in our dataset or those from already published repositories is heterogeneity regarding the patients' conditions, their treatment, the exact timing of sample collection, and potentially others. We have sought to express such potential confounders wherever indicated.

As we observed distinct changes in IgM aPL, and less so in IgG or IgA, an emerging question might be whether these aPL display a propensity

towards seroconversion. The assumption, then, would be that IgG and IgA increase with time, while IgM would show an inclination to waning. We have investigated this question from multiple angles and found no evidence for seroconversion from IgM to IgA or to IgG. However, when looking at the global dataset, the IgM levels did not drop even after >200 DPO, which indicates that these IgM are more than a transient phenomenon post infection with SARS-CoV-2. But what are the factors, other than infection with SARS-CoV-2, that are associated with aPL levels? To answer this question, we have first identified relevant features using a random forest and have then built a GLM, to identify and validate the relevant parameters. The most salient factor was anti-SARS-CoV-2 NC IgG, which emerged as determinant for PT, AnV,  $\beta$ 2GPI IgM, and for CL IgG, suggesting that the strength of the antibody response after infection with SARS-CoV-2, more than after vaccination, modulates these aPL. Age was an additional covariate which, in combination with other parameters, showed correlation. While this confirms previous findings [18], the modulatory effect of various cytokines we had reported here would require additional validation for the evidence to be considered strong. In general, cytokine profiles have not been given much attention in the antiphospholipid field and systematic assessments are lacking to date. In this regard, our dataset provided here will be a valuable resource to compare the cytokine (but also aPL) profiles in our cohorts with those of patients with primary or secondary APS.

Finally, we aimed to identify correlates of thrombotic complications. While any parameter could be associated with it and may be identified, we formulated the hypothesis that – given the evidence presented above – the occurrence of aPL in COVID-19 is correlated with a higher incidence of thromboses. While this would still not prove a mechanistic causation, it would make a strong case for it. However, our approach combining four analytic modalities failed in detecting evidence for correlation between aPL and thromboses in COVID-19. This could be because in the APS, many identified more significant correlations with thrombosis for the IgG than for IgM aPL, albeit a minority of studies reported significant associations with thrombosis for IgM but not IgG antibodies [83]. Moreover, it was shown in a recent report that the detection of IgM aPL is of added diagnostic value in obstetric but not thrombotic APS [84]. But are there other factors that might be predictive of thrombotic insults? The hypersecretion of inflammatory cytokines and chemokines as a result of the cytokine storm syndrome contributes to complement and coagulation cascade activation, to disseminated intravascular coagulation, and ultimately, to thrombotic complications [66,85]. Indeed, we identified that a pro-inflammatory signature (our inflammatory index), together with few other cytokines and chemokines like G-CSF and IL-6 may be contributing factors. Yet, the unambiguously most important predictor of thromboses was disease severity and, partially overlapping, the antibody response against SARS-CoV-2. This result is not surprising as COVID-19 is associated with coagulopathy and thrombotic complications, particularly in severe disease [3,7,8,86,87]. Along these lines, microthrombi are frequently diagnosed only post-mortem and we would have missed them, which poses a limitation.

The most apparent limitation of our endeavour, however, is the lack of validation cohorts. The creation of an independent COVID-19 cohort, or a comparison cohort with another respiratory infectious disease, with available data on thrombotic events and a deep molecular characterisation, including antibodies against SARS-CoV-2 and large cytokine and aPL panels, is laborious. However, we have taken all conceivable steps to remedy this lack: (1) To some extent, the current study can be viewed as an extension of our previous work [18] where we identified the strength of the antibody response against SARS-CoV-2 proteins to be a main driver of aPL levels, and where we identified the same candidates to be enriched as here. In this regard, the present study already served as a validation cohort of our recent undertakings. (2) In agreement with this, whenever possible, we have included publicly available data, to compare our findings. Thus, independent controls have been inserted on multiple occasions in the study. (3) We have welcomed complexity in

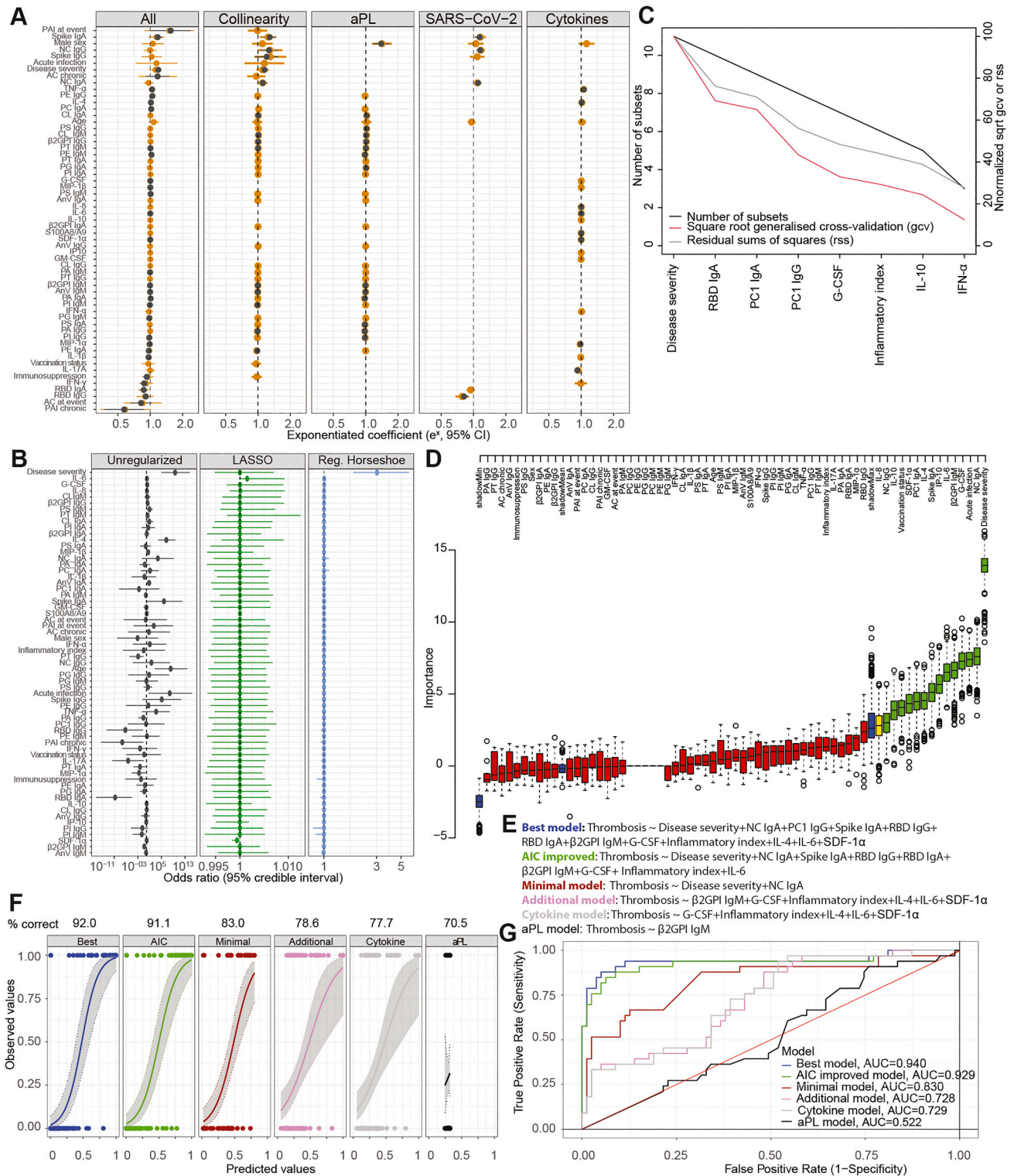


**Fig. 7.** Thrombotic events are mainly associated with SARS-CoV-2 disease severity and evidence for association with aPL is strongly limited and likely non-existent. We applied several regression models for the identification of potentially relevant parameters correlated with the occurrence of thromboses. A. Shown are the data for conventional linear multivariable regression for all and selected features, with (dark grey) and without (yellow) AIC improvement. The exponentiated regression coefficient with the respective 95% confidence interval is shown. B. Bayesian multivariable logistic regression model. Three priors were used and compared: an unregularised prior, a LASSO, and a regularised horseshoe. Disease severity showed an odds ratio of 2.98 (CrI95%: 1.80-5.81) and stood out as the most correlated parameter when using the regularised horseshoe shrinkage prior. C. A multiadaptive regression spline model (MARS) was used, tuned for binomial outcome data. Disease severity emerged as the most correlated feature with thrombosis. D. Random forest regression with Boruta suggested that disease severity is the most correlated parameter with thrombosis. E. Based on consensus information from all four regression methodologies, we selected the most important parameters and built models with them. The equations are displayed here. F. Model-based predicted probabilities for the occurrence of thrombosis are compared with the observed occurrences. G. ROC curves with respective AUC values for each of the models. (For interpretation of the references to colour in this figure legend, the reader is referred to the web version of this article.)



**Table 7**  
List of features predicting thromboses.

	Ordinary multivariable linear regression	Bayesian multivariable logistic regression	MARS	Boruta
Thrombosis ~	Disease severity, NC IgG, NC IgA, Spike IgG, Spike IgA	Disease severity, IL-6, SDF-1 $\alpha$	Disease severity, RBD IgA, PC1 IgA, PC1 IgG, G-CSF, Inflammatory index, IL-10, IFN- $\alpha$	Disease severity, NC IgA, acute infection, G-CSF, $\beta$ 2GPI IgM, IL-6, IP-10, Spike IgA, IL-4, PC1 IgA, SDF-1 $\alpha$ , vaccination status, IL-10, NC IgG, IL-8

our dataset and have accounted for it. Conversely, the incentives to exclude heterogeneity in cohort-based studies, to make the findings more robust, often result in a lack of generalisability [88,89], questioning the relevance of the finding for the larger, heterogeneous population. (4) We have been cautious when interpreting the results and have provided extensive contextualisation. Moreover, we provided detailed descriptions of the methods and made the code used to conduct the analyses fully available.

Ultimately, there can be many incentives to not only observe and describe associations but to ascribe causality. In the heat of the SARS-CoV-2 pandemic when rapid learning was paramount, many erudite speculations turned into rapid shots, fired without having a clear vision. While idleness may oppose progress, hasty conclusions, perhaps appearing attractive, bear a danger, too, by disseminating questionable knowledge as factual under the umbrella of science. In this regard, the pandemic may have contributed to understanding the importance of being aware of our own ignorance, our *docta ignorantia* [90], which builds the foundation of our scientific aspiration.

## Funding

This work was supported by the Driver Grant 2017DRI17 of the Swiss Personalized Health Network, by grants of Innovation Fund of the University Hospital Zurich (INOV00096), and of the NOMIS Foundation, the Schwyzer Winiker Stiftung, and the Baugarten Stiftung (coordinated by the USZ Foundation, USZF27101) to ME as well as Swiss National Science Foundation Starting Grant 211422, University of Zurich CRPP Precision medicine for bacterial infections, and USZ Foundation USZF270808 to SDB.

## Author statement

Conceptualisation: VE, ME  
 Data curation: ME  
 Formal analysis: ME  
 Funding acquisition: SDB, ME  
 Investigation: SDB, SMS, TCS, AGM, CCC, TB, KBMF, DR, PDWG, PKB  
 Methodology: ME, SDB, SMS  
 Supervision: ME  
 Visualisation: ME  
 Writing - original draft: ME  
 Writing - review and editing: VE, SDB, DR, KBMF, TCS, PDWG, PKB, SMS, AGM, CCC, TB

## Declaration of Competing Interest

DR has a management role and is a shareholder of GA Generic Assays GmbH and Medipan GmbH but no financial conflict of interest. Both companies are diagnostic manufacturers. TB is an employee of Generic Assays GmbH. All other authors declare no competing interest.

## Data availability

Specific data sets can be shared upon reasonable request and if an approval by an ethics committee as well as a data transfer agreement is in place. •

Code used in this study is publicly available on Zenodo [62]. •

Any additional information required to reanalyse the data reported in this paper is available from the lead contact ([marc.emmenegger@usb.ch](mailto:marc.emmenegger@usb.ch)) upon request.

## Acknowledgements

We are grateful to all the patients who enabled this study by means of signing the hospital-wide general consent and thereby contributed to scientific understanding. In general, it is our experience that the general public is extremely supportive of patient-based medical research, of whose outcomes they will ultimately benefit. VE and ME conceived the study and wrote part of the manuscript in fond memory of their beloved teacher and dear friend, Hansruedi Isler (1934-2019), whose inspiration exceeds a lifetime.

## Appendix A. Supplementary data

Supplementary data to this article can be found online at <https://doi.org/10.1016/j.clim.2023.109845>.

## References

- [1] Y. Zuo, S.K. Estes, R.A. Ali, A.A. Gandhi, S. Yalavarthi, H. Shi, G. Sule, K. Gockman, J.A. Madison, M. Zuo, V. Yadav, J. Wang, W. Woodard, S.P. Lezak, N.L. Lugogo, S. A. Smith, J.H. Morrissey, Y. Kanthi, J.S. Knight, Prothrombotic autoantibodies in serum from patients hospitalized with COVID-19, *Sci. Transl. Med.* 12 (2020), <https://doi.org/10.1126/SCITRANSLMED.ABD3876>.
- [2] E.M. Conway, N. Mackman, R.Q. Warren, A.S. Wolberg, L.O. Mosnier, R. A. Campbell, L.E. Gralinski, M.T. Rondina, F.L. van de Veerdonk, K.M. Hoffmeister, J.H. Griffin, D. Nugent, K. Moon, J.H. Morrissey, Understanding COVID-19-associated coagulopathy, *Nat. Rev. Immunol.* 22 (2022) 639–649, <https://doi.org/10.1038/s41577-022-00762-9>, 2022 22:10.
- [3] D.A. Gorog, R.F. Storey, P.A. Gurbel, U.S. Tantry, J.S. Berger, M.Y. Chan, D. Duerschmied, S.S. Smyth, W.A.E. Parker, R.A. Ajjan, G. Vilahur, L. Badimon, J. M. ten Berg, H. ten Cate, F. Peyvandi, T.T. Wang, R.C. Becker, Current and novel biomarkers of thrombotic risk in COVID-19: a consensus statement from the international COVID-19 thrombosis biomarkers colloquium, *Nat. Rev. Cardiol.* 19 (2022) 475–495, <https://doi.org/10.1038/s41569-021-00665-7>, 2022 19:7.
- [4] J. Hippisley-Cox, M. Patone, X.W. Mei, D. Saatci, S. Dixon, K. Khunti, F. Zaccardi, P. Watkinson, M. Shankar-Hari, J. Doidge, D.A. Harrison, S.J. Griffin, A. Sheikh, C. A.C. Coupland, Risk of thrombocytopenia and thromboembolism after COVID-19 vaccination and SARS-CoV-2 positive testing: self-controlled case series study, *BMJ* 374 (2021), <https://doi.org/10.1136/bmj.n1931>.
- [5] V. Mai, B.K. Tan, S. Mainbourg, F. Potus, M. Cucherat, J.C. Lega, S. Provencher, Venous thromboembolism in COVID-19 compared to non-COVID-19 cohorts: a systematic review with meta-analysis, *Vasc. Pharmacol.* 139 (2021), 106882, <https://doi.org/10.1016/j.vph.2021.106882>.
- [6] J. Snell, SARS-CoV-2 infection and its association with thrombosis and ischemic stroke: a review, *Am. J. Emerg. Med.* 40 (2021) 188–192, <https://doi.org/10.1016/j.ajem.2020.09.072>.
- [7] F.K. Ho, J.P. Pell, Thromboembolism and bleeding after COVID-19, *BMJ* (2022), <https://doi.org/10.1136/bmj.O817>.
- [8] I. Katsoularis, O. Fonseca-Rodríguez, P. Farrington, H. Jerndal, E.H. Lundevaller, M. Sund, K. Lindmark, A.M. Fors Connolly, Risks of deep vein thrombosis, pulmonary embolism, and bleeding after COVID-19: nationwide self-controlled cases series and matched cohort study, *BMJ* 377 (2022), e069590, <https://doi.org/10.1136/bmj-2021-069590>.
- [9] E. Korompoki, M. Gavriatopoulou, D. Fotiou, I. Ntanas-Stathopoulos, M. A. Dimopoulos, E. Terpos, Late-onset hematological complications post COVID-19: an emerging medical problem for the hematologist, *Am. J. Hematol.* 97 (2022) 119–128, <https://doi.org/10.1002/AJH.26384>.





- [53] B. Carpenter, A. Gelman, M.D. Hoffman, D. Lee, B. Goodrich, M. Betancourt, M. A. Brubaker, J. Guo, P. Li, A. Riddell, Stan: a probabilistic programming language, *J. Stat. Softw.* 76 (2017), <https://doi.org/10.18637/jss.v076.i01>.
- [54] B. Goodrich, J. Gabry, I. Ali, S. Brilleman, Rstanarm: Bayesian Applied Regression Modeling Via Stan. <https://mc-stan.org/rstanarm>, 2020 (accessed February 1, 2021).
- [55] D. Lamparter, R.P.B. Jacquat, J. Riou, D. Menges, T. Ballouz, M. Emmenegger, Code Repository for SARS-CoV-2 Seroprevalence Study, 2022, <https://doi.org/10.5281/ZENODO.7454292>.
- [56] M. Losa, M. Emmenegger, P. De Rossi, P.M. Schuerch, T. Serdiuk, N. Pengo, D. Capron, D. Bieli, N.J. Rupp, M.C. Carta, K.J. Frontzek, V. Lysenko, R. Reimann, A.K. Lakkaraju, M. Nuvolone, G.T. Westermark, K.P. Nilsson, M. Polymenidou, A. P. Theocharides, S. Hornemann, P. Picotti, A. Aguzzi, The ASC Inflammasome Adapter Controls the Severity of Inflammation-Related AA Amyloidosis, *BioRxiv*, 2023, <https://doi.org/10.1101/2021.05.01.442282>, 2021.05.01.442282.
- [57] J. Piironen, A. Vehtari, Sparsity information and regularization in the horseshoe and other shrinkage priors, *Electron. J. Stat.* 11 (2017) 5018–5051, <https://doi.org/10.1214/17-EJS1337SI>.
- [58] J.H. Friedman, Multivariate Adaptive Regression Splines, *Doi:https://doi.org/10.1214/Aos/1176347963* 19, 1991, pp. 1–67, <https://doi.org/10.1214/AOS/1176347963>.
- [59] S. Milborrow, Earth: Multivariate Adaptive Regression Splines. <http://CRAN.R-project.org/package=earth>, 2011.
- [60] M.D. Wilkinson, M. Dumontier, I.J. Aalbersberg, G. Appleton, M. Axton, A. Baak, N. Blomberg, J.W. Boiten, L.B. da Silva Santos, P.E. Bourne, J. Bouwman, A. J. Brookes, T. Clark, M. Crosas, I. Dillo, O. Dumon, S. Edmunds, C.T. Evelo, R. Finkers, A. Gonzalez-Beltran, A.J.G. Gray, P. Groth, C. Goble, J.S. Grethe, J. Heringa, P.A.C.T. Hoern, R. Hooft, T. Kuhn, R. Kok, J. Kok, S.J. Lusher, M. E. Martone, A. Mons, A.L. Packer, B. Persson, P. Rocca-Serra, M. Roos, R. van Schaik, S.A. Sansone, E. Schultes, T. Sengstag, T. Slater, G. Strawn, M.A. Swertz, M. Thompson, J. Van Der Lei, E. Van Mulligen, J. Velterop, A. Waagmeester, P. Wittenburg, K. Wolstencroft, J. Zhao, B. Mons, The FAIR guiding principles for scientific data management and stewardship, *Sci. Data* 3 (2016) 1–9, <https://doi.org/10.1038/sdata.2016.18>, 2016 3:1.
- [61] R. Van Noorden, Medicine is plagued by untrustworthy clinical trials. How many studies are faked or flawed? *Nature* 619 (2023) 454–458, <https://doi.org/10.1038/D41586-023-02299-W>.
- [62] M. Emmenegger, V. Emmenegger, Code Repository for Antiphospholipid Antibodies are Enriched Post-Acute COVID-19 but do not Modulate the Thrombotic Risk, 2023, <https://doi.org/10.5281/zenodo.10051978>.
- [63] A.M. Wendelboe, G.E. Raskob, Global burden of thrombosis, *Circ. Res.* 118 (2016) 1340–1347, <https://doi.org/10.1161/CIRCRESAHA.115.306841>.
- [64] M. Gatto, C. Perricone, M. Tonello, O. Bistoni, A.M. Cattelan, R. Bursi, G. Cafaro, E. De Robertis, A. Mencacci, S. Bozza, A. Vianello, L. Iaccarino, R. Gerli, A. Doria, E. Bartoloni, Frequency and clinical correlates of antiphospholipid antibodies arising in patients with SARS-CoV-2 infection: findings from a multicentre study on 122 cases, *Clin. Exp. Rheumatol.* 38 (2020) 754–759. <http://www.ncbi.nlm.nih.gov/pubmed/32723434> (accessed October 30, 2021).
- [65] M.Y. Najem, F. Couturaud, C.A. Lemarié, Cytokine and chemokine regulation of venous thromboembolism, *J. Thromb. Haemost.* 18 (2020) 1009–1019, <https://doi.org/10.1111/JTH.14759>.
- [66] A. Wolf, F. Khimani, B. Yoon, C. Gerhart, D. Endsley, A.K. Ray, A.F. Yango, S. D. Flynn, G.Y.H. Lip, S.A. Gonzalez, M. Sathyamoorthy, The mechanistic basis linking cytokine storm to thrombosis in COVID-19, *Thromb. Update* 8 (2022), 100110, <https://doi.org/10.1016/J.TRU.2022.100110>.
- [67] H.O. Kim, H.S. Kim, J.C. Youn, E.C. Shin, S. Park, Serum cytokine profiles in healthy young and elderly population assessed using multiplexed bead-based immunoassays, *J. Transl. Med.* 9 (2011) 113, <https://doi.org/10.1186/1479-5876-9-113>.
- [68] P.A. Mudd, J.C. Crawford, J.S. Turner, A. Souquette, D. Reynolds, D. Bender, J. P. Bosanquet, N.J. Anand, D.A. Striker, R.S. Martin, A.C.M. Boon, S.L. House, K. E. Remy, R.S. Hotchkiss, R.M. Presti, J.A. O'Halloran, W.G. Powderly, P. G. Thomas, A.H. Ellebedy, Distinct inflammatory profiles distinguish COVID-19 from influenza with limited contributions from cytokine storm, *Sci. Adv.* 6 (2020), <https://doi.org/10.1126/sciadv.abe3024>.
- [69] Y. Li, J.S. Yi, M.A. Russo, M. Rosa-Bray, K.J. Weinhold, J.T. Guptill, Normative dataset for plasma cytokines in healthy human adults, *Data Brief* 35 (2021), 106857, <https://doi.org/10.1016/J.DIB.2021.106857>.
- [70] J.S. Kwon, J.Y. Kim, M.C. Kim, S.Y. Park, B.N. Kim, S. Bae, H.H. Cha, J. Jung, M. J. Kim, M.L. Jin, S.H. Choi, J.W. Chung, E.C. Shin, S.H. Kim, Factors of severity in patients with COVID-19: cytokine/chemokine concentrations, viral load, and antibody responses, *Am. J. Trop. Med. Hyg.* 103 (2020) 2412–2418, <https://doi.org/10.4269/AJTMH.20-1110>.
- [71] A. Perperoglou, W. Sauerbrei, M. Abrahamowicz, M. Schmid, A review of spline function procedures in R, *BMC Med. Res. Methodol.* 19 (2019) 1–16, <https://doi.org/10.1186/S12874-019-0666-3>, 2019 19:1.
- [72] J. Gauthier, Q.V. Wu, T.A. Gooley, Cubic splines to model relationships between continuous variables and outcomes: a guide for clinicians, *Bone Marrow Transplant.* 55 (2019) 675–680, <https://doi.org/10.1038/s41409-019-0679-x>, 2019 55:4.
- [73] E. Shikova, V. Reshkova, A. Kumanova, S. Saleva, D. Alexandrova, N. Capó, M. Murovska, B. On, Cytomegalovirus, Epstein-Barr virus, and human herpesvirus-6 infections in patients with myalgic encephalomyelitis/chronic fatigue syndrome, *J. Med. Virol.* 92 (2020) 3682, <https://doi.org/10.1002/JMV.25744>.
- [74] M. Ruiz-Pablos, B. Paiva, R. Montero-Mateo, N. Garcia, A. Zabaleta, Epstein-Barr virus and the origin of myalgic encephalomyelitis or chronic fatigue syndrome, *Front. Immunol.* 12 (2021) 4637, <https://doi.org/10.3389/FIMMU.2021.656797/BIBTEX>.
- [75] P. Magnus, N. Gunnes, K. Tveito, I.J. Bakken, S. Ghaderi, C. Stoltenberg, M. Hornig, W.I. Lipkin, L. Trogstad, S.E. Håberg, Chronic fatigue syndrome/myalgic encephalomyelitis (CFS/ME) is associated with pandemic influenza infection, but not with an adjuvanted pandemic influenza vaccine, *Vaccine* 33 (2015) 6173–6177, <https://doi.org/10.1016/J.VACCINE.2015.10.018>.
- [76] D. Menges, T. Ballouz, A. Anagnostopoulos, H.E. Aschmann, A. Domenghino, J. S. Fehr, M.A. Puhán, Burden of post-COVID-19 syndrome and implications for healthcare service planning: a population-based cohort study, *PLoS One* 16 (2021), e0254523, <https://doi.org/10.1371/journal.pone.0254523>.
- [77] S.J. Yong, Long COVID or post-COVID-19 syndrome: putative pathophysiology, risk factors, and treatments, *Infect. Dis. Ther.* 53 (2021) 737–754, <https://doi.org/10.1080/23744235.2021.1924397>.
- [78] T. Iba, J.H. Levy, J.M. Connors, T.E. Warkentin, J. Thachil, M. Levi, The unique characteristics of COVID-19 coagulopathy, *Crit. Care* 24 (2020) 1–8, <https://doi.org/10.1186/s13054-020-03077-0>.
- [79] T. Iba, T.E. Warkentin, J. Thachil, M. Levi, J.H. Levy, Proposal of the definition for COVID-19-associated coagulopathy, *J. Clin. Med.* 10 (2021) 191, <https://doi.org/10.3390/jcm10020191>.
- [80] O. Vollmer, C. Tacquard, Y. Dieudonné, B. Nespolo, L. Sattler, L. Grunebaum, V. Gies, M. Radosavljevic, C. Kaeuffer, Y. Hansmann, J.-C. Weber, T. Martin, L. Arnaud, O. Morel, A. Guffroy, O. Collange, P.M. Mertes, A.-S. Korganow, X. Delabranche, V. Poindron, Follow-up of COVID-19 patients: LA is transient but other aPLs are persistent, *Autoimmun. Rev.* 20 (2021), 102822, <https://doi.org/10.1016/j.autrev.2021.102822>.
- [81] O. Hasan Ali, D. Bomze, L. Risch, S.D. Brugger, M. Paprotny, M. Weber, S. Thiel, L. Kern, W.C. Albrich, P. Kohler, C.R. Kahlert, P. Vernazza, P.K. Bühler, R. A. Schüpbach, A. Gómez-Mejía, A.M. Popa, A. Bergthaler, J.M. Penninger, L. Flatz, Severe coronavirus disease 2019 (COVID-19) is associated with elevated serum immunoglobulin (Ig) A and antiphospholipid IgA antibodies, *Clin. Infect. Dis.* 73 (2021) e2869–e2874, <https://doi.org/10.1093/CID/CIAB1496>.
- [82] R.J. Hsu, W.C. Yu, G.R. Peng, C.H. Ye, S.Y. Hu, P.C.T. Chong, K.Y. Yap, J.Y.C. Lee, W.C. Lin, S.H. Yu, The role of cytokines and chemokines in severe acute respiratory syndrome coronavirus 2 infections, *Front. Immunol.* 13 (2022) 1109, <https://doi.org/10.3389/FIMMU.2022.832394/BIBTEX>.
- [83] H. Kelchtermans, L. Pelkmans, B. de Laat, K.M. Devreese, IgG/IgM antiphospholipid antibodies present in the classification criteria for the antiphospholipid syndrome: a critical review of their association with thrombosis, *J. Thromb. Haemost.* 14 (2016) 1530–1548, <https://doi.org/10.1111/JTH.13379>.
- [84] W. Chayoua, H. Kelchtermans, J.C. Gris, G.W. Moore, J. Musiał, D. Wahl, P.G. de Groot, B. de Laat, K.M.J. Devreese, The (non-)sense of detecting anti-cardiolipin and anti- $\beta$ 2glycoprotein I IgM antibodies in the antiphospholipid syndrome, *J. Thromb. Haemost.* 18 (2020) 169–179, <https://doi.org/10.1111/JTH.14633>.
- [85] L. Yang, X. Xie, Z. Tu, J. Fu, D. Xu, Y. Zhou, The signal pathways and treatment of cytokine storm in COVID-19, *Signal Transduct. Target. Ther.* 6 (2021) 1–20, <https://doi.org/10.1038/s41392-021-00679-0>, 2021 6:1.
- [86] R. Knight, V. Walker, S. Ip, J.A. Cooper, T. Bolton, S. Keene, R. Denholm, A. Akbari, H. Abbaszanjani, F. Torabi, E. Omigie, S. Hollings, T.L. North, R. Toms, X. Jiang, E. Di Angelantonio, S. Denaxas, J.H. Thygesen, C. Tomlinson, B. Bray, C.J. Smith, M. Barber, K. Khunti, G.D. Smith, N. Chaturvedi, C. Sudlow, W.N. Whiteley, A. M. Wood, J.A.C. Sterne, Association of COVID-19 with major arterial and venous thrombotic diseases: a population-wide cohort study of 48 million adults in England and Wales, *Circulation* 146 (2022) 892–906, <https://doi.org/10.1161/CIRCULATIONAHA.122.060785>.
- [87] J. Loo, D.A. Spittle, M. Newnham, COVID-19, immunothrombosis and venous thromboembolism: biological mechanisms, *Thorax* 76 (2021) 412–420, <https://doi.org/10.1136/THORAXJNL-2020-216243>.
- [88] A.F. Marquand, I. Rezek, J. Buitelaar, C.F. Beckmann, Understanding heterogeneity in clinical cohorts using normative models: beyond case-control studies, *Biol. Psychiatry* 80 (2016) 552–561, <https://doi.org/10.1016/J.BIOPSYCH.2015.12.022>.
- [89] J.P.A. Ioannidis, Why most clinical research is not useful, *PLoS Med.* 13 (2016), <https://doi.org/10.1371/JOURNAL.PMED.1002049>.
- [90] N. de Cusa, De docta ignorantia, *Meiner, Hamburg*, p. 1440.